esa

ECOSPHERE

Predator ontogeny determines trophic cascade strength in freshwater rock pools

JUNIPER L. SIMONIS[1,†]

Department of Ecology and Evolutionary Biology, Cornell University, Ithaca, New York 14853 USA

Citation: Simonis, J. L. 2013. Predator ontogeny determines trophic cascade strength in freshwater rock pools. Ecosphere 4(5):62. http://dx.doi.org/10.1890/ES13-00019.1

Abstract. Ontogenetic changes in consumers can influence the magnitude and outcome of direct and indirect ecological interactions. Although most research has focused on the consequences of qualitative changes in diet (i.e., shifts in trophic guild between life-history stages), quantitative effects of ontogeny, such as size-dependent per capita consumption rates, likely also influence food webs by modulating the relative importance of top-down control. I examined the effect of predator ontogeny on per capita consumption rates, selectivity between prey species, and the resulting food-web consequences using a system of freshwater rock pools on Appledore Island, Maine, USA. The rock pools house a simple tri-trophic food chain consisting of chlorophyte algae consumed by cladoceran grazers (*Moina macrocopa* and *Daphnia pulex*), which are then preyed upon by the aquatic insect *Trichocorixa verticalis* (Corixidae). Laboratory studies showed that *Trichocorixa* grows substantially during its life history, with size-dependent (i.e., allometric) increases in per capita predation rates (consuming both *Moina* and *Daphnia*). Predation rates were significantly higher on *Moina* than *Daphnia* in single-prey experiments and all instars of *Trichocorixa* significantly preferred *Moina* in choice experiments. In a mesocosm experiment, predation by *Trichocorixa* on zooplankters created a top-down trophic cascade by releasing phytoplankton from grazing and the strength of the cascade increased significantly with *Trichocorixa* life-history stage. A yearlong observational study of three rock pools in the field indicated that top-down interactions are present and strongly affect food-web dynamics in situ, as well. In particular, time-series modeling showed that increases in *Trichocorixa* biomass (due to ontogenetic growth and hatching) led to decreases in *Moina* population growth rates, which caused increases in phytoplankton population growth rates. Taken together, these results indicate that consumer ontogeny can affect food-web and ecosystem dynamics without qualitative niche shifts if per capita feeding rates change substantially over the consumer's life history. Given the prevalence of both allometrically scaling consumption rates and dynamically structured predator populations, top-predator demography may be an important driver of the trophic structure and dynamics of food webs.

Key words: allometric scaling; consumption rate; Isles of Shoals Archipelago; life history; multivariate auto-regressive state-space model; *Moina macrocopa*; prey choice; stage-structured predator; rock pool; top-down control; *Trichocorixa verticalis*.

Received 17 January 2013; revised 13 April 2013; accepted 23 April 2013; **published** 29 May 2013. Corresponding Editor: J. Benstead.

Copyright: © 2013 Simonis. This is an open-access article distributed under the terms of the Creative Commons Attribution License, which permits unrestricted use, distribution, and reproduction in any medium, provided the original author and source are credited. http://creativecommons.org/licenses/by/3.0/

[1] Present address: Alexander Center for Applied Population Biology, Department of Conservation and Science, Lincoln Park Zoo, Chicago, Illinois 60614 USA.

† **E-mail:** jsimonis@lpzoo.org

Introduction

Most animal species grow substantially as they develop from newborn (neonate) to adult (Peters 1983, Werner 1988), and many key ecological and physiological parameters, such as per capita consumption rate and metabolism, scale allometrically with body size (Mittelbach 1981, Peters 1983, Kooijman 1993, Brown et al. 2004). As a result, the strengths and outcomes of ecological interactions may change as a function of the size distributions of interacting species (Werner and Gilliam 1984, Persson 1987, Persson et al. 1998, Cohen et al. 2003, Hildrew et al. 2007*a*). At the extreme, ontogenetic changes result in individuals qualitatively shifting their diet or habitat use at a critical point in their life history (e.g., metamorphosis), a phenomenon that is known as an ontogenetic niche shift (Werner and Gilliam 1984) and can have significant effects on the dynamics of populations, food webs, and ecosystems (Polis and Strong 1996, Woodward and Hildrew 2002, Rudolf 2007, Rudolf and Lafferty 2011). However, even if individuals do not shift their diet or niche qualitatively as they grow, individual growth often results in important quantitative changes in vital rates (Kooijman 1993, Brown et al. 2004) which may influence the strength of ecological interactions.

In particular, many predators show strong increases in per capita consumption rates as they develop and grow (Thompson 1975, Mittelbach 1981, Peters 1983, Shine 1991, Kooijman 1993, Aljetlawi et al. 2004). Although common, increased consumption with size is not universal among predators: some species show negative or hump-shaped relationships between individual size and per capita consumption rate (e.g., Persson 1987, Byström and Andersson 2005). Regardless of the specific relationship between size and consumption, any ontogenetic change in the per capita predation rate may influence population and food-web dynamics by altering the strength of the predator-prey trophic link and the relative importance of top-down control in the food web (Alford 1989, de Roos et al. 2003). However, the broader ecological effects of any ontogenetic changes in individual vital rates depend upon the size-structure of the population, particularly whether it is stable or dynamic (Kooijman 1993).

For example, if the size structure of a predator population is stable, the overall rate of consumption by the population will depend only on population density, even if larger predators consume more prey items per capita. Conversely, if the size distribution of the predator population is dynamic (e.g., due to non-overlapping generations or size-dependent mortality rates) and individuals display an ontogenetic change in predation rate, the overall rate of consumption will fluctuate as a function of the size distribution of individuals, even if the population size remains constant. As a result, consumer demography may play an important role in dictating the dynamics of consumer-resource interactions by causing fluctuations in predation strength and may even introduce novel, destabilizing feedbacks between consumer populations and their resources (de Roos et al. 1990, Persson et al. 1998, de Roos and Persson 2002, de Roos et al. 2003). Given the complexity of ecosystems, however, the trophic consequences of predator ontogeny and related changes in individual consumption rates will likely depend upon the food-web context in which the consumer-resource interaction occurs (Hairston and Hairston 1997, Hildrew et al. 2007*b*, Jones and Jeppesen 2007).

In a simple food chain with three trophic levels, consumption by the top predator is predicted to decrease the density of intermediate consumers, potentially indirectly increasing the biomass of the basal resource via a trophic cascade (Hairston et al. 1960, Paine 1980, Strong 1992, Polis 1999, Schmitz et al. 2000, Shurin et al. 2002). It may therefore be expected that more voracious predators with stronger trophic links (higher per capita predation rates) will cause stronger trophic cascades, all else being equal (Paine 1980, Pace et al. 1999). Indeed, variation in consumption rates among apex predators is a major factor influencing the presence and strength of trophic cascades across ecosystems (Hairston and Hairston 1993, Polis 1999, Borer et al. 2005, Hambright et al. 2007). Similarly, ontogenetically driven variation in a particular top predator's consumption rate may shift the relative importance of top-down and bottom-up control within the food chain and determine if a trophic cascade occurs in that ecosystem. However, despite the near ubiquity of ontogenetic growth of consumers and relationships between

21508925, 2013, 5, Downloaded from https://esajournals.onlinelibrary.wiley.com/doi/10.1890/ES13-00019.1, Wiley Online Library on [22/01/2026]. See the Terms and Conditions (https://onlinelibrary.wiley.com/terms-and-conditions) on Wiley Online Library for rules of use; OA articles are governed by the applicable Creative Commons License

body size and per capita consumption rate, the effects of ontogenetic changes in predator consumption rates on trophic dynamics within ecosystems remain poorly studied (de Roos et al. 2003).

Here I examine the role of predator ontogeny, and thus size, on the rate of predation and the strength of top-down control in a system of freshwater rock pools on Appledore Island, Maine, USA. The pools contain a simple tritrophic food chain of phytoplankton (primarily chlorophyte algae) consumed by herbivorous zooplankton (primarily *Moina macrocopa* and *Daphnia pulex* [Cladocera, Daphniidae]) which are in turn preyed upon by *Trichocorixa verticalis* (Hemiptera, Corixidae) (J. G. Morin et al., *unpublished data*). *Trichocorixa* is a potentially voracious consumer (Wurtsbaugh 1992) that grows substantially in size during its ontogeny (Kelts 1979; see also *Results*). Adult *Trichocorixa* prey strongly enough upon *Artemia* (brine shrimp) in the Great Salt Lake, USA to release phytoplankton from grazing pressure and cause a trophic cascade (Wurtsbaugh 1992). However, little else is known about the trophic ecology of this geographically widely distributed and highly invasive aquatic insect (Tones and Hammer 1975, Tones 1977, Kelts 1979, Wurtsbaugh and Berry 1990, van de Meutter et al. 2010).

Putatively a "generalist omnivore" (Kelts 1979), *Trichocorixa* possesses piercing and sucking mouthparts typical of Hemiptera that make it capable of consuming a wide range of resources (e.g., filamentous algae, zooplankton, dipertan larvae). In the rock pools studied here, Cladocera (*Moina* in particular) are by far the most abundant and available prey for *Trichocorixa*, as filamentous algae are not found in the pools and the chironomid larvae present construct protective cases that deter predation (Dillon 1985; J. L. Simonis, *personal observation*). By comparison, the cladocerans are widely distributed among pools and often reach densities exceeding 1,000 individuals/L (Simonis 2012) due to the high productivity of the pools (Loder et al. 1996). However, the cascading effects of *Trichocorixa* predation on the food web likely depends upon which cladocerans are present in the rock pool, as the two species display widely different intrinsic rates of population growth (*Moina* reproduces much more quickly than *Daphnia*; J. L. Simonis, *unpublished data*). It is also possible that older *Trichocorixa* supplement their diet by cannibalizing younger individuals, a widespread phenomenon among the Corixidae (Pajunen and Pajunen 1991), but there are no published data regarding cannibalism in this species and I have not observed it in any of my studies (including experiments designed to test for cannibalism; J. L. Simonis, *personal observation*).

The goals of this study were to determine the effect of top-predator ontogeny on predation rate and trophic dynamics in the Appledore rockpool ecosystem. I used laboratory feeding experiments to show that all life history stages of *Trichocorixa* consume both prey species (*Daphnia* and *Moina*), yet prefer *Moina*, and that per capita consumption rates scale allometrically with predator body size. This increase in predation rate with ontogeny led to a significant increase in the strength of top-down control in a mesocosm experiment. The trophic effect of *Trichocorixa* ontogeny was evident in unmanipulated rock pools as well, as increased *Trichocorixa* biomass (when *Trichocorixa* developed into adults and after the second generation hatched) led to decreased zooplankton population growth rates and caused a cascading increase in phytoplankton population growth rates. These results indicate that even without a qualitative shift in feeding niche, top predator ontogeny can influence food-web structure and trophic dynamics.

Methods

Study system

Trichocorixa is an aquatic insect that is native to saline and freshwater habitats across North America (Tones and Hammer 1975, Tones 1977, Kelts 1979, Wurtsbaugh and Berry 1990) and has also invaded wetlands in Iberia, Africa, and New Caledonia (Jansson 1982, Sala and Boix 2005, van de Meutter et al. 2010). Its ontogeny includes seven life-history stages: egg, five juvenile instars (each lasting 5–10 days), and adult. *Trichocorixa* overwinters as eggs, hatching commences in spring or early summer, and there are typically two or three partially-overlapping generations per year, resulting in a dynamic population age structure (Tones 1977, Kelts 1979; see also *Results*). Individuals grow substantially over their ontogeny from approximately 1 mm (body

21508925, 2013, 5, Downloaded from https://esajournals.onlinelibrary.wiley.com/doi/10.1890/ES13-00019.1, Wiley Online Library on [22/01/2026]. See the Terms and Conditions (https://onlinelibrary.wiley.com/terms-and-conditions) on Wiley Online Library for rules of use; OA articles are governed by the applicable Creative Commons License

length) as first-instar juveniles to approximately 5 mm as adults (Kelts 1979; see also *Results*). On the Isles of Shoals Archipelago (Gulf of Maine, USA), *Trichocorixa* is commonly found in freshwater rock pools that sit above the high tide line. Appledore, the largest island in the archipelago and home to the Shoals Marine Laboratory (SML), is 38.5 ha with approximately 1,500 rock pools, which range in size from ca. 1.0 to 30,000 L. The Appledore pools contain a relatively simple food web that is dominated by a tritrophic food chain of chlorophyte algae, consumed by *Moina* and *Daphnia*, which are, in turn, preyed upon by *Trichocorixa* (J. G. Morin et al., *unpublished data*). Although other species of aquatic invertebrates are found in the pools (e.g., chironomids, ostracods, and cyclopoid copepods), the most abundant prey for *Trichocorixa* are cladocerans, and in particular, *Moina* (Simonis 2012).

All *Trichocorixa* used in experiments reported here were collected from rock pools on Appledore Island in May and June 2009, held in 20-L plastic buckets in the laboratory at SML, and fed ad libitum on a mixture of *Daphnia* and *Moina*. Individual *Trichocorixa* used in the experiments were identified to instar based on body shape, size, color, and wing development, following Kelts (1979). Separate laboratory cultures of *Daphnia* and *Moina* for use as prey in experiments were maintained in 20-L buckets and fed rock-pool phytoplankton.

Characterizing predator and prey sizes

To determine the length and weight of each non-egg *Trichocorixa* life-history stage, I removed 22 individuals of each instar from the laboratory culture, starved them for 24 hours (in individual vials), and then freeze-killed them at −20°C. I measured each individual's length, using digital calipers under a dissecting microscope, and dry weight (dried at 60°C for 48 hours) using an ultra-micro balance (Sartorius SE2). I fit a standard length-weight regression to the data using non-linear least squares regression in R (R Development Core Team 2011) and determined the average size of each instar. I also used the laboratory cultures to determine the average sizes of *Daphnia* and *Moina*. I photographed 20 non-gravid female individuals of each species under a dissecting microscope (4–10× magnification), measured their lengths using ImageJ software (Abramoff et al. 2004), and converted the lengths to dry weights using published relationships (McCauley 1984).

Functional response experiments

I used a set of functional response experiments to quantify predation rates and determine how they are influenced by predator age class and prey species identity. Single *Trichocorixa* individuals of known instar were placed into glass jars containing 100 mL of filtered (0.45 μm) well water and non-gravid, adult female prey of either *Daphnia* or *Moina*. To standardize hunger levels among predators, I starved the *Trichocorixa* for 24 hours before each feeding trial. Prey abundances used were 1, 2, 4, 8, 10, 12, 15, 20, 25, 30, 40, 50, 75, and 100 individuals per jar, giving densities between 10 and 1,000 prey/L, which spans most of the range seen in the Appledore rock pools (Simonis 2012). Experimental jars were placed in a temperature-stable room (mean: 18°C, range: 16–20°C) with fluorescent lamps ("plant and aquarium", Phillips 40W) on a 12:12 light:dark cycle. After 24 hours, I removed the predators using a wide-bore pipette and enumerated the remaining prey by filtering the contents of each jar through a 30-μm mesh sieve and loading the retained sample into a counting tray. I did not replace prey during the trials and no predators or prey were re-used between trials. I conducted duplicate trials for each of the six predator instars at each of the 14 prey densities for the two prey species, giving 336 total trials.

I fit the data using the Rogers Random Predator Equation, which is a Type-II functional response adapted to account for depletion of prey during feeding (Rogers 1972):

$$N = N_0\left(1 - e^{a(Nh - PT)}\right) \qquad (1a)$$

where N is the number of prey eaten out of the initial number of prey available (N_0), a and h are the baseline attack rate and handling time, P is the number of predators (here, $P = 1$), and T is the total time (here, $T = 24$ h). I adapted Eq. 1a to test if either handling time or attack rate changed with predator ontogeny by allowing both a and h to scale allometrically with predator mass (using the average dry mass for each instar). I also tested if there were differences between the

21508925, 2013, 5, Downloaded from https://esajournals.onlinelibrary.wiley.com/doi/10.1890/ES13-00019.1, Wiley Online Library on [22/01/2026]. See the Terms and Conditions (https://onlinelibrary.wiley.com/terms-and-conditions) on Wiley Online Library for rules of use; OA articles are governed by the applicable Creative Commons License

functional responses for the two prey species by allowing all parameters to differ between the two prey species (via a dummy variable approach). Thus, the attack rate in Eq. 1a is actually

$$a = (a_i + d \times \Delta a_i) \times m^{(a_s + d \times \Delta a_s)} \quad (1b)$$

where a_i is the intercept attack rate when consuming *Moina*, a_s is the scaling effect of predator mass (m) on attack rate when consuming *Moina*, d is the dummy variable to account for prey species identity (equal to 0 when prey were *Moina*, equal to 1 when prey were *Daphnia*), and Δa_i and Δa_s are the differences in the intercept and scaling parameters, respectively, between *Daphnia* and *Moina* prey items. Similarly, the handling time in Eq. 1a is

$$h = (h_i + d \times \Delta h_i) \times m^{(h_s + d \times \Delta h_s)} \quad (1c)$$

where h_i is the intercept handling time when consuming *Moina*, h_s is the scaling effect of predator mass (m) on handling time when consuming *Moina*, d is the dummy variable to account for prey species identity (equal to 0 when prey were *Moina*, equal to 1 when prey were *Daphnia*), and Δh_i and Δh_s are the differences in the intercept and scaling parameters, respectively, between *Daphnia* and *Moina* prey items.

Model fitting was conducted using maximum likelihood and the mle2 function in the R package bbmle (Bolker and R Development Core Team 2011), and the significance of each parameter was determined using Likelihood Ratio Tests (LRTs) based on corrected AIC (AICc) values. Note, however, that N (the number of prey eaten) is on both sides of Eq. 1a, and in particular is in an exponential function on the right-hand side, meaning that Eq. 1 does not have a simple closed-form solution. Following McCoy and Bolker (2008), I solved Eq. 1 using the Lambert W function, which works appropriately with standard maximum likelihood-based approaches.

Prey choice experiment

I determined the preference of each *Trichocorixa* instar for the two prey species (*Daphnia* and *Moina*) using a choice experiment. Predators of known instar were starved for 24 hours, then placed singly into glass jars containing 200 mL of filtered (0.45 μm) well water and 20 non-gravid, adult females each of *Daphnia* and *Moina* (40 cladocerans total, the only density used). The jars were placed in the same temperature and light conditions as for the functional response experiments. After 24 hours, I removed the predators and counted the remaining prey (following method used for the functional response experiments). I conducted ten replicate trials for each *Trichocorixa* instar, for 60 total trials. I did not replace prey during the trials nor reuse any predators or prey.

I quantified predator preference using the Chesson-Manly alpha metric (hereafter: α_{CM}; Manly 1974, Chesson 1978) with Manly's (1974) approximation to account for prey depletion. The expected value of α_{CM} under no preference with two prey types is 0.50 for both species, if predators attack the prey types equally. However, *Trichocorixa* have a much higher predation rate on *Moina* than *Daphnia* (see *Results*, attack rate on *Moina* is 2.84 × attack rate on *Daphnia*), perhaps due to differences in size or behavior between prey species. Accounting for the difference in attack rates, I recalculated the expected value of α_{CM} to be 0.74 for *Moina* and 0.26 for *Daphnia* (following the methods of Chesson 1983, which are appropriate for situations with prey depletion). I calculated the selectivity of each *Trichocorixa* instar towards *Moina* and evaluated the significance of these selectivities using *t*-tests with a null expected value of 0.74. I also regressed α_{CM} against instar to determine if selectivity changed with ontogeny.

Food web mesocosm experiment

I then used a mesocosm experiment to determine if predation by *Trichocorixa* is strong enough to affect zooplankton population densities and cascade to indirectly affect phytoplankton biomass, and if the age-structure of the *Trichocorixa* population mediates the strength of the cascade. Four *Trichocorixa* treatment levels were used: predators absent, small juveniles (second and third instars), large juveniles (fourth and fifth instars), and adults. I chose these treatment levels to reflect the age structure typically seen in field *Trichocorixa* populations (multiple similar-aged juvenile instars present simultaneously and adults often without juveniles present; Tones 1977, Kelts 1979; see also *Results*), but I excluded first-instar *Trichocorixa* in this experiment due to their high mortality rates (see *Results*). In July

21508925, 2013, 5, Downloaded from https://esajournals.onlinelibrary.wiley.com/doi/10.1890/ES13-00019.1, Wiley Online Library on [22/01/2026]. See the Terms and Conditions (https://onlinelibrary.wiley.com/terms-and-conditions) on Wiley Online Library for rules of use; OA articles are governed by the applicable Creative Commons License

2009, I collected and combined water from five representative rock pools around Appledore Island. I filtered (30 μm) the water, removing all macrozooplankton and *Trichocorixa*, but leaving microzooplankton and phytoplankton. Mesocosms (40-L Rubbermaid totes) were placed outdoors in full sunlight and arranged in a 4 × 4 grid, then filled with 30 L of the rock-pool water mixture that had an initial phytoplankton density of 800 μg chlorophyll-*a*/L and a salinity of 0.4 ppt. The temperature of the water was 16.8°C when the mesocosms were set up, but it fluctuated with weather during the course of the experiment (noontime water temperature ranged from 16.3 to 28.5°C, mean: 22.2°C). I then inoculated all of the mesocosms with a mixture of zooplankton from the same five pools (supplemented with individuals from the zooplankton laboratory cultures) to create initial densities of 40 *Daphnia*/L and 125 *Moina*/L. These phytoplankton and zooplankton densities are within the range of rock pools on Appledore (Simonis 2012; and see *Results*).

The mesocosm communities were left to equilibrate for four days before the *Trichocorixa* treatment was established. To minimize any among-mesocosm variation that might have developed during these four days, I removed 5 L from each mesocosm, combined and homogenized this volume in a large bucket, removed a small volume (1 L total) to quantify chlorophyll and zooplankton densities (methods described below), and redistributed the remaining volume equally back among the mesocosms. I then added fifteen *Trichocorixa* individuals (0.5 *Trichocorixa*/L) to each of the predator-present mesocosms according to the treatment levels outlined above. For the two juvenile predator treatment levels, each replicate had the same instar composition, determined by availability in the laboratory culture ("small juvenile": 10 second-instar and five third-instar individuals, "large juvenile": five fourth-instar and 10 fifth-instar individuals). Each treatment level was replicated four times and the treatment levels were arranged spatially in a 4 × 4 Latin Square design. I covered all of the mesocosms with 1 mm mesh screening to prevent any immigration or emigration by *Trichocorixa* or other organisms and reinforced the mesh with chicken wire to exclude gulls (*Larus* spp.). The experiment ran for 12 days after the addition of *Trichocorixa*, which likely encompassed three generations of the dominant prey species, *Moina* (Nandini and Sarma 2000). I checked the mesocosms every three days and removed and replaced any *Trichocorixa* that had molted out of their treatment-level instar class or had died.

On the final day of the experiment, I sampled the mesocosms for phytoplankton and zooplankton densities. Prior to sampling, I gently stirred the mesocosms to homogenize the water column without resuspending flocculent detritus. I sampled chlorophyll-*a* as a proxy for phytoplankton biomass (Wetzel and Likens 2000) by collecting duplicate water samples from each mesocosm and filtering them onto glass-fiber filters (Whatman GF-F), with a pre-filtration step using a 75-μm sieve to remove zooplankton. The GF-F filters were kept frozen and dark until analyzed. I extracted chlorophyll-*a* from the filters in the dark for 24 hours in cold ethanol (90%) and measured fluorescence on a desktop fluorometer (Turner Designs TD-700), with HCl acidification to correct for phaeopigments (Nusch 1980). To estimate zooplankton densities, I filtered each mesocosm in its entirety through a 75-μm mesh and preserved the contents in 95% ethanol until I counted them under a dissecting microscope. When necessary due to high densities, I subsampled the zooplankton samples following standard protocols (Wetzel and Likens 2000). The reported and analyzed grazer densities were for total cladocerans (*Moina* and *Daphnia* together), due to the very low densities of *Daphnia* in all mesocosms (see *Results*).

I analyzed the phytoplankton and zooplankton data using separate ANOVAs to determine the overall significance of the *Trichocorixa* effect and incorporating two independent a priori contrasts (Gotelli and Ellison 2004) to address my specific, directional hypotheses. The first contrast tested whether the presence of *Trichocorixa* (of any instar) induced a trophic cascade. That is, did the three treatment levels with *Trichocorixa* present have significantly lower densities of zooplankton and significantly higher densities of phytoplankton than the no-*Trichocorixa* controls? The second contrast used a linear ordered term to test if older instars caused significantly stronger top-down effects. That is, did later instar treatment levels have significantly lower zoo-

21508925, 2013, 5, Downloaded from https://esajournals.onlinelibrary.wiley.com/doi/10.1890/ES13-00019.1, Wiley Online Library on [22/01/2026]. See the Terms and Conditions (https://onlinelibrary.wiley.com/terms-and-conditions) on Wiley Online Library for rules of use; OA articles are governed by the applicable Creative Commons License

plankton densities and significantly higher phytoplankton densities? Both the zooplankton and phytoplankton data were $\log_{10}$-transformed prior to analyses to homogenize variances and normalize residuals. I conducted the ANOVAs (with a priori contrasts) in R (R Development Core Team 2011).

Trophic dynamics in the field

Finally, I explored the trophic consequences of *Trichocorixa* predation and ontogeny in situ by sampling a set of three rock pools every 2–4 days from 22 May to 15 August 2009 (29 sample dates). At each pool on a sample date, I collected duplicate 500 mL samples haphazardly from throughout the water column using a large-bulb pipette with a 5.0 mm diameter orifice, removed all invertebrates from the water via a 75-μm mesh sieve, and preserved the plankton in 95% ethanol until I enumerated the samples under a dissecting microscope. If any species were present in high densities, I counted replicate representative subsamples. I also identified all *Trichocorixa* present to instar, based on size and morphology (Kelts 1979; see also *Results*), and determined the total biomass of for *Trichocorixa* in each sample using the length-weight regression (see *Results*). I estimated phytoplankton biomass in all three pools on each sample date by collecting duplicate small volumes of water from each pool (typically <25 mL), which I processed using the chlorophyll-*a* methods as described for the mesocosm experiment. Duplicate samples were averaged (and converted to densities per L) to generate one datum for each trophic level in each pool on each sample date. I also measured the temperature, dissolved oxygen concentration, salinity, and pH of the pools on each sample date using a YSI 556 Multi-probe and estimated each pool's volume, assuming basins were shaped as inverted cones (following Pajunen and Pajunen 2007). The volumes of the three pools were approximately 175, 305, and 350 L (see *Results*), thus each plankton sampling removed only ~0.3–0.6% of any population present at that time. I analyzed the resulting field data using a multivariate autoregressive state-space model (MARSS; Ives et al. 2003, Holmes et al. 2012) to determine if the trophic interactions observed in the experiments were detectable in situ. The MARSS approach allows one to estimate species interaction strengths from time-series data and a typical model includes two components: a state-process model, which describes changes in population sizes due to ecological interactions and environmental covariates, and an observation-process model, which introduces observation error associated with incomplete sampling of the populations (Ives et al. 1999, Ives et al. 2003, Holmes et al. 2012).

The state-process model I used relates the population density of each trophic level at time t ($\mathbf{x}_t$) to the density of all trophic levels (including itself) at time $t - \tau$ (where τ is a time lag, here always $\tau = 1$) via interaction strengths $\mathbf{B}$ and to covariates at time t ($\mathbf{c}_t$) via parameters $\mathbf{C}$:

$$\mathbf{x}_t = \mathbf{B}\mathbf{x}_{t-1} + \mathbf{u} + \mathbf{C}\mathbf{c}_t + \mathbf{w}_t \quad \text{where } \mathbf{w}_t \sim \text{MVN}(0, \mathbf{Q}) \tag{2a}$$

in compact matrix notation (see Appendix A for the full model form). Here, $\mathbf{u}$ are intercepts (one for each trophic level) and $\mathbf{w}_t$ are process errors that are multivariate normal (MVN) with mean 0 and covariance matrix $\mathbf{Q}$. Because the state-process model (Eq. 2a) relates the populations at time $t = 1$ to the populations at time $t = 0$, their states at time $t = 0$ ($\mathbf{x}_0$) must be estimated. Here, I treated the initial conditions of the states as fixed but unknown parameters $\boldsymbol{\pi}$, such that $\mathbf{x}_0 \equiv \boldsymbol{\pi}$. The true, but unknown, states $\mathbf{x}_t$ are then passed through the observation-process model, which relates them to the observed values of the populations at time t ($\mathbf{y}_t$) by introducing observation errors $\mathbf{v}_t$ (multivariate normal with mean 0 and covariance matrix $\mathbf{R}$):

$$\mathbf{y}_t = \mathbf{x}_t + \mathbf{v}_t \quad \text{where } \mathbf{v}_t \sim \text{MVN}(0, \mathbf{R}). \tag{2b}$$

Rather than fit the $\mathbf{R}$ terms (observation variances) in the MARSS model, I estimated them externally by determining the average coefficient of variation among the duplicate samples taken on each date (following Carpenter et al. 1994). This resulted in observation variances of 0.007 (phytoplankton), 0.10 (*Moina*), and 0.30 (*Trichocorixa*), which are similar to other published values for sampling planktonic organisms (Carpenter et al. 1994).

To accommodate the irregular sampling regime, I modeled the data using a fixed time step of one day, covering 86 calendar days, with observations only occurring on the 29 sample dates. I treated the three pools as independent

21508925, 2013, 5, Downloaded from https://esajournals.onlinelibrary.wiley.com/doi/10.1890/ES13-00019.1, Wiley Online Library on [22/01/2026]. See the Terms and Conditions (https://onlinelibrary.wiley.com/terms-and-conditions) on Wiley Online Library for rules of use; OA articles are governed by the applicable Creative Commons License

replicates and included them in a single model with a common set of **B**, **C**, **Q**, and **R** parameters, but with independent **u** parameters and initial states **π** (see Appendix A). All state variable data were log-transformed prior to analyses and the covariate data were untransformed, meaning that the entries in **B** and **C** can be interpreted as the effects of the (log) abundance of species *j* on the population growth rate of species *i* and the effects of each covariate on each species' population growth rate, respectively. To be included as true covariates (and not as state variables), environmental parameters need to have data for all days modeled, not just the sample dates. I therefore linearly interpolated each environmental parameter to estimate their values on the 57 unobserved dates. Further, to make $\mathbf{x}_t$ dependent on $\mathbf{c}_{t-1}$ (the time lag on which population densities influence each other) rather than $\mathbf{c}_t$ (the default of the MARSS model; Eq. 2a), I offset the covariate data forward one day (following Holmes et al. 2012), necessitating a one-day backward extrapolation to estimate $\mathbf{c}_0$ and avoid dropping data, which I did using the rate from the first interpolation (see Appendix A).

The environmental covariates I considered for the time-series analysis were temperature, dissolved oxygen concentration, pH, and salinity. However, temperature, dissolved oxygen, and pH were all strongly correlated ($\rho_{\text{temp-DO}} = 0.63$, $\rho_{\text{temp-pH}} = 0.68$, $\rho_{\text{DO-pH}} = 0.81$; all $P < 0.001$), likely reflecting that sunny days increase both water temperature and photosynthesis, photosynthesis raises O_2 and lowers CO_2 concentrations, and lower CO_2 leads to higher pH due to the low buffering capacity of the pools. Temperature was the most predictive of those three covariates in single-covariate versions of the model (data not shown), and so only temperature and salinity were included as covariates in the full model evaluation. The fullest possible model therefore included nine parameters in **B** (all pairwise species interactions in both directions and the three autoregressive terms), six parameters in **C** (temperature and salinity independently influencing each of the three trophic levels), nine parameters in **u** and nine parameters in **π** (separate intercepts and $\mathbf{x}_0$ for each trophic level in each pool), and three parameters in **Q** (one process variance for each trophic level), for a total of 36 parameters (see Appendix A). The simplest possible model included 24 parameters: **u**, **π**, and **Q** as they were in the fullest model, but with **B** only including the three autoregressive parameters and **C** empty. I determined the best-fitting model structure using stepwise model selection (both addition and deletion of parameters) based on AICc scores and starting from both the fullest and simplest possible models. The MARSS models were fit in the MARSS package in R (Holmes et al. 2012) using the expectation-maximization (EM) algorithm to find the maximum likelihood parameter estimates (Holmes 2012).

Results

Predator and prey sizes

Trichocorixa grew substantially during its ontogeny, with individuals approximately doubling their mass at each of the five molts (Appendix B: Fig. B1; dry weight $= 0.0059 \times \text{length}^{3.078}$; 92% of deviance explained). First-instar juveniles weighed 0.020 ± 0.002 mg (dry weight) and measured 1.24 ± 0.02 mm (max length), whereas adults were nearly 45 times heavier and over four times longer at 0.864 ± 0.070 mg and 5.07 ± 0.09 mm (all data means ± SEM, N = 22 individuals per instar). The size of the prey used in the experiments was both consistent within, and quite different between, the two species (Appendix B: Fig. B1), with *Daphnia* (0.053 ± 0.003 mg, 2.02 ± 0.05 mm, mean ± SEM, N = 20) being substantially larger than *Moina* (0.012 ± 0.001 mg, 1.23 ± 0.02 mm, mean ± SEM, N = 20). As a result, individuals from the two prey species potentially represented large differences in energetic rewards for the predator, depending on conversion efficiencies. Also, *Trichocorixa* individuals grow through the size spectrum of their prey: first-instar *Trichocorixa* are nearly identical in size to *Moina* but not until the third instar were individual predators larger than *Daphnia* (Appendix B: Fig. B1). This overlap in predator and prey sizes does not necessarily preclude consumption, as *Trichocorixa* uses piercing mouth parts to fluid-feed on its prey and so is not limited by mouth gape size. However, the predator-prey size overlap could still influence the ability of different predator instars to capture and subdue their prey.

21508925, 2013, 5, Downloaded from https://esajournals.onlinelibrary.wiley.com/doi/10.1890/ES13-00019.1, Wiley Online Library on [22/01/2026]. See the Terms and Conditions (https://onlinelibrary.wiley.com/terms-and-conditions) on Wiley Online Library for rules of use; OA articles are governed by the applicable Creative Commons License

Functional response experiments

All six instars of *Trichocorixa* were able to feed on both prey species and the functional response curves describing this predation took a saturating (Type II) shape (Fig. 1). Attack rate and handling time both had significant intercept values (Table 1; $a_i = 0.068$ 1/h, $h_i = 0.270$ h, both $P < 0.001$) and scaled allometrically: attack rate increased and handling time decreased as functions of predator mass ($a_s = 0.482$ 1/(h·mg), $h_s = -0.620$ h/mg, both $P < 0.001$). Three of the four parameters differed significantly between the prey species, all showing increased predation rates on *Moina* (Tables 1 and 2). *Trichocorixa* had a lower attack rate intercept and a higher handling time intercept when preying upon *Daphnia* compared with *Moina* (respectively, $\Delta a_i = -0.044$ 1/h, $P < 0.001$; $\Delta h_i = 0.270$ h, $P = 0.007$) and *Trichocorixa*'s handling time decreased less rapidly with increasing predator biomass when consuming *Daphnia* compared with *Moina* ($\Delta h_s = 0.210$ h, $P = 0.044$). The scaling of attack rate with predator mass did not significantly differ between the prey species (Δa_s; $P > 0.05$).

Although per capita predation was much higher on *Moina* than on *Daphnia* for all six *Trichocorixa* instars (Fig. 1, Table 2), the total mass of *Daphnia* consumed was substantially higher than the total mass of *Moina* consumed, a result of the size difference between the prey species (*Daphnia* is 4.4 times larger than *Moina* in dry weight; Appendix B: Fig. B1). Consequently, mass-specific consumption (mass of prey consumed ÷ mass of predator) was much higher for *Trichocorixa* of all instars when preying upon *Daphnia* than when preying upon *Moina* (Table 2). Despite the increase in the number of prey consumed with predator ontogeny, the increase in prey mass consumed by each instar was less than the growth in predator biomass between instars, causing predator mass-specific consumption to decrease monotonically with increasing instar (Table 2).

Prey choice experiment

When given both prey species together, *Trichocorixa* strongly preferred *Moina* over *Daphnia* (across all predator instars, α_{CM} for *Moina* = 0.930 ± 0.014, mean ± SEM, N = 60) and all six *Trichocorixa* instars displayed significant preference for *Moina*, even after accounting for the difference in their attack rates between the two prey species (Fig. 2A; $P < 0.001$ for the first four juvenile instars, $P = 0.026$ for fifth-instar juveniles, $P = 0.019$ for adults). Despite all predator instars preferring *Moina*, older *Trichocorixa* were significantly less selective towards *Moina* than were younger individuals (regression of α_{CM} against instar, slope = −0.032, $P < 0.001$). As expected given the functional responses (Fig. 1, Tables 1 and 2), older predators consumed significantly more prey individuals in total (Poisson regression of total prey eaten against instar, slope = 0.18, $P < 0.001$). There was also a significant positive correlation between the number of *Moina* and the number of *Daphnia* eaten (Fig. 2B; $r = 0.45$, $P < 0.001$).

Food web mesocosm experiment

The *Trichocorixa* treatment had significant effects on the densities of both cladoceran grazers ($F_{3,12} = 4.53$, $P = 0.02$) and phytoplankton ($F_{3,12} = 3.66$, $P = 0.04$) in the mesocosm experiment (Fig. 3). Regardless of instar, the presence of *Trichocorixa* led to a decrease in the density of cladocerans and an increase in the density of phytoplankton (a priori contrasts between treatment levels with and without *Trichocorixa*, cladocerans: contrast = −0.116, $P = 0.009$; phytoplankton: contrast = 0.074, $P = 0.024$; Fig. 3). Further, the strength of both responses was significantly greater in the treatments containing later life-history stages of the predators (a priori linear contrasts among treatments with *Trichocorixa*, cladocerans: contrast = −0.344, $P = 0.019$; phytoplankton: contrast = 0.207, $P = 0.049$; Fig. 3). In the absence of predators, the density of cladocerans increased and phytoplankton decreased significantly from the pre-*Trichocorixa* densities (dashed lines in Fig. 3; *t*-tests with null expected values equal to the initial values; both $P < 0.05$), indicating that the zooplankton can reach high enough densities to suppress phytoplankton population growth rates. This effect also appeared to occur over the four day equilibration period before the addition of *Trichocorixa*, during which zooplankton concentrations increased from 165 to 223 individuals/L and phytoplankton concentrations dropped from 800 to 719 μg chlorophyll-*a*/L (data not shown). Any change in phytoplankton density observed in the mesocosms was likely not the result of excretion by predators or

21508925, 2013, 5, Downloaded from https://esajournals.onlinelibrary.wiley.com/doi/10.1890/ES13-00019.1, Wiley Online Library on [22/01/2026]. See the Terms and Conditions (https://onlinelibrary.wiley.com/terms-and-conditions) on Wiley Online Library for rules of use; OA articles are governed by the applicable Creative Commons License

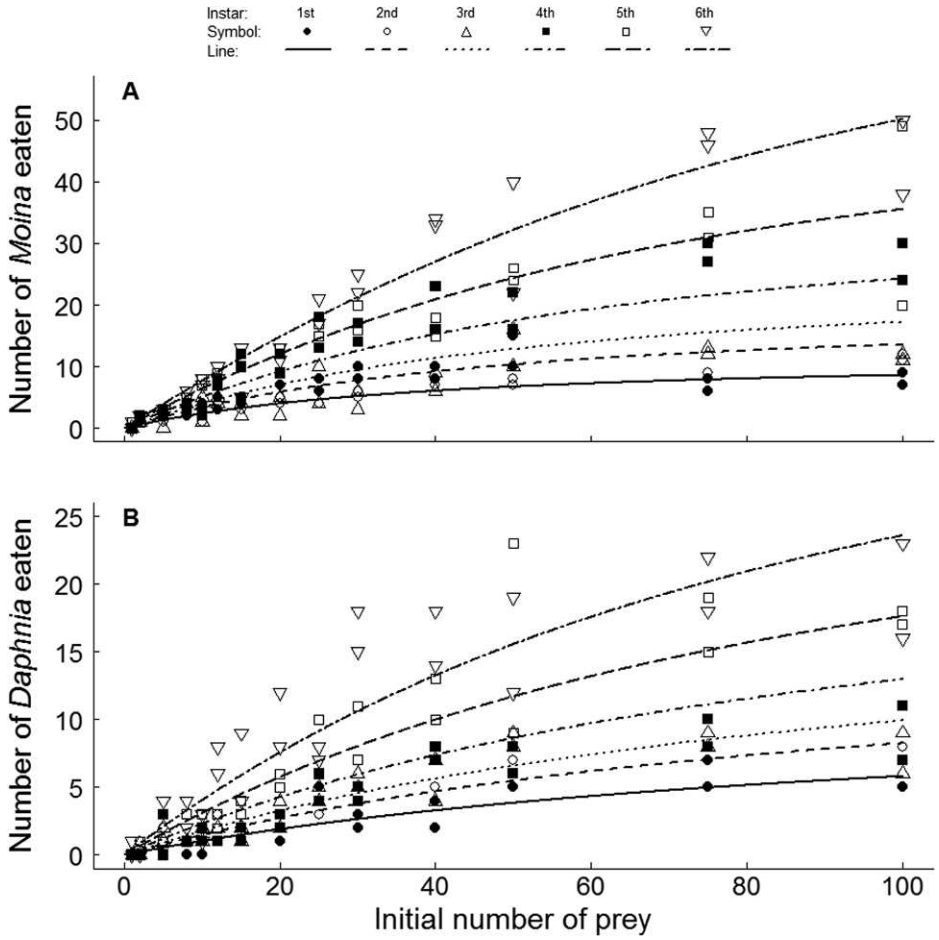

Fig. 1. Functional responses for each of six *Trichocorixa* instars feeding on (A) *Moina* or (B) *Daphnia*. All data were fit with a single model based on the Rogers Random Predator Equation with allometric scaling of parameters across instars and differences in all parameters between prey species (Eq. 1 and Table 1). Note the difference in *y*-axes between (A) and (B).

grazers, since nutrient concentrations are extremely high in the Appledore rock pool water as the result of a steady input of gull guano (Sze 1981, Loder et al. 1996).

Despite the strong preference of *Trichocorixa* for *Moina* and the higher rate of predation on *Moina* compared to *Daphnia*, all of the mesocosms were dominated by *Moina* at the end of the experiment. Indeed, *Daphnia* was only found in three of the mesocosms and always at much lower densities than *Moina*. There was no clear relationship between the *Trichocorixa* treatment level and the presence of *Daphnia*: they were found in one mesocosm containing adult predators (17 *Daphnia*/L) and two containing small juvenile predators (1 and 2 *Daphnia*/L). This decrease in *Daphnia* densities appears to have begun before the predator treatment was imposed: during the four day equilibration period, the density of *Daphnia* decreased from 40 to 18 individuals/L (compared to an increase in *Moina* from 125 to 205 individuals/L). This suggests that some aspect of the mesocosm environment was unfavorable for *Daphnia*. One likely factor may have been the high phytoplankton densities, as *Daphnia* is not commonly found in rock pools with over 250 μg chlorophyll-*a*/L (J. L. Simonis, *unpublished data*). Also present in the mesocosms were *Brachionus* (rotifer), *Acanthocyclops* (copepod), and chironomid larvae. However, these

21508925, 2013, 5, Downloaded from https://esajournals.onlinelibrary.wiley.com/doi/10.1890/ES13-00019.1, Wiley Online Library on [22/01/2026]. See the Terms and Conditions (https://onlinelibrary.wiley.com/terms-and-conditions) on Wiley Online Library for rules of use; OA articles are governed by the applicable Creative Commons License

Table 1. Best fit parameters from the functional response model where both attack rate and handling time were allowed to scale allometrically with predator biomass and the resulting four parameters could differ between prey species (Eq. 1).

Parameter	Estimate†	SE	P
a_i	0.068	0.005	<0.001
Δa_i	−0.044	0.005	<0.001
a_s	0.482	0.039	<0.001
h_i	0.270	0.030	<0.001
Δh_i	0.270	0.010	0.007
h_s	−0.620	0.059	<0.001
Δh_s	0.210	0.104	0.044

Notes: The scaling term for attack rate (a_s) did not differ significantly between the prey species (Δa_s; LRT, $P > 0.05$) and thus was removed from the model. Translation of these parameters into instar- and prey-specific functional response parameters is shown in Table 2.

†Units were 1/h for attack rates and h for handling time.

taxa were generally at low densities (<40 individuals/L) and none displayed changes in density significantly associated with the predator treatment (data not shown).

Trophic dynamics in the field

All three pools surveyed had populations of chlorophyte algae, *Moina*, and *Trichocorixa*, but no *Daphnia* (Fig. 4). There were also populations of *Brachionus* and chironomid larvae in all three pools. However, the chironomids were at relatively low densities (average: 8.6 chironomids/L) and typically in protective cases attached to the benthos, which prevent predation by *Trichocorixa* (J. L. Simonis, *personal observation*). The survey began when the first generation of *Trichocorixa* was in the third through fifth instars and lasted through the hatching and partial development of the second generation (Appendix B: Fig. B2). The first generation reached adulthood 2–2.5 weeks into the survey and the second generation began hatching approximately three weeks later (Appendix B: Fig. B2). *Trichocorixa* population densities were relatively constant at near 5 individuals/L during the survey period, except when the population densities temporarily exploded (ca. Julian Date 190–210, maximum of 116 *Trichocorixa*/L) due to the hatching of the second generation (Appendix B: Fig. B2). However, the second *Trichocorixa* generation appears to have experienced high mortality among the youngest instars, as population densities decreased markedly in the weeks following the hatching and there was relatively low recruitment to later-

Table 2. Estimated parameters for functional response curves of each *Trichocorixa* instar consuming each prey species (Fig. 1) as fitted using the allometric model shown in Table 1.

Prey	Instar	Average Corixid mass (mg dry wt)	Attack rate (1/h)	Handling time (h)	Predicted prey eaten†		Predicted DSC‡ (%)
					No.	Mass (mg dry wt)	
Moina	1	0.038	0.014	2.05	8.61	0.104	273.8
Moina	2	0.085	0.021	1.25	13.61	0.165	193.7
Moina	3	0.130	0.025	0.96	17.25	0.209	160.9
Moina	4	0.241	0.034	0.65	24.27	0.294	121.8
Moina	5	0.495	0.048	0.42	35.55	0.430	87.0
Moina	6	0.992	0.068	0.27	50.18	0.607	61.2
Daphnia	1	0.038	0.005	2.08	5.81	0.307	806.3
Daphnia	2	0.085	0.007	1.49	8.26	0.436	513.2
Daphnia	3	0.130	0.009	1.25	9.93	0.524	404.0
Daphnia	4	0.241	0.012	0.97	12.97	0.685	284.0
Daphnia	5	0.495	0.017	0.72	17.61	0.930	188.1
Daphnia	6	0.992	0.024	0.54	23.58	1.245	125.5

† The predicted number and dry weight of prey eaten (in 24 hours) was determined using the functional responses with 100 initial prey individuals.

‡ Predicted daily specific consumption (Predicted DSC) was calculated as the predicted mass of prey eaten in 24 hours divided by the average mass of the *Trichocorixa* instar and is displayed as a percentage.

21508925, 2013, 5, Downloaded from https://esajournals.onlinelibrary.wiley.com/doi/10.1890/ES13-00019.1, Wiley Online Library on [22/01/2026]. See the Terms and Conditions (https://onlinelibrary.wiley.com/terms-and-conditions) on Wiley Online Library for rules of use; OA articles are governed by the applicable Creative Commons License

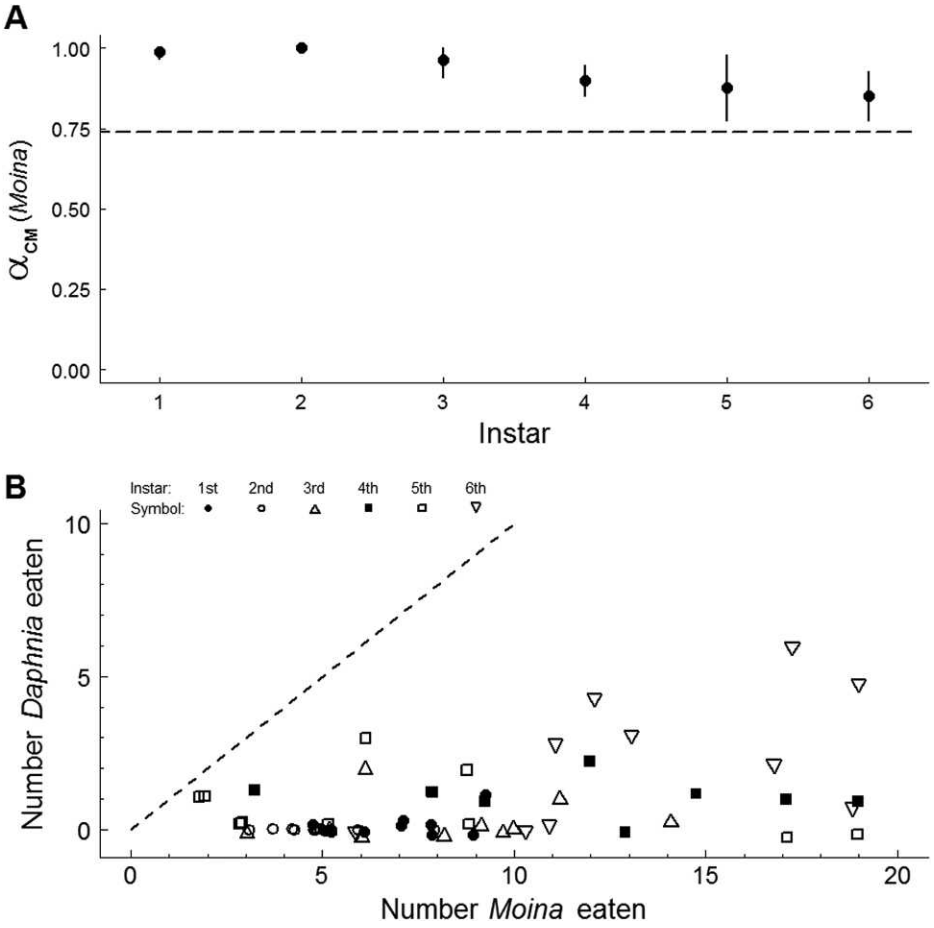

Fig. 2. *Trichocorixa* choice between prey species (*Daphnia* and *Moina*) across *Trichocorixa* instars. (A) Preference of each *Trichocorixa* instar for *Moina* (as measured by α_{CM}; points are means with 95% CIs) in relation to the expected value given the differences in attack rates on the two species (dashed horizontal line; $\alpha_{CM} = 0.74$). (B) Individual predator data showing the relationship between the number of prey consumed from each species. Data in (B) were slightly jittered in both the *x*- and *y*-directions and the 1:1 line was added to aid interpretation. Note the different ranges for the *x*- and *y*-axes.

instar stages (Fig. 4A, Appendix B: Fig. B2). As a result of these changes in total population size and size-structure, the biomass of *Trichocorixa* generally increased during the beginning of the survey, peaked during the hatching of the second generation, and decreased at the end of the survey (Fig. 4A, Appendix B: Fig. B2). Conversely, *Moina* densities in all three pools were high at the beginning of the survey, decreased during the middle of the survey (after *Trichocorixa* populations became dominated by adults), and increased again later in the summer following the mass mortality of the second generation of *Trichocorixa* (Figs. 4B, 5). The decrease in *Moina* density was also followed by the expected increase in phytoplankton density (Figs. 4C, 5), reflecting the trophic cascade seen in the mesocosm experiment (Fig. 3). Both the predator-grazer and grazer-phytoplankton relationships displayed similar dynamics among the three pools, as shown by their trajectories in the consumer-resource phase planes (Fig. 5). And despite any differences among pools (e.g., varying densities at the beginning of the experiment, or offset timing of *Trichocorixa* maturation), the temporal dynamics of all three trophic levels were synchronized among the pools: average cross-correlation coefficients were 0.69 for the

21508925, 2013, 5, Downloaded from https://esajournals.onlinelibrary.wiley.com/doi/10.1890/ES13-00019.1, Wiley Online Library on [22/01/2026]. See the Terms and Conditions (https://onlinelibrary.wiley.com/terms-and-conditions) on Wiley Online Library for rules of use; OA articles are governed by the applicable Creative Commons License

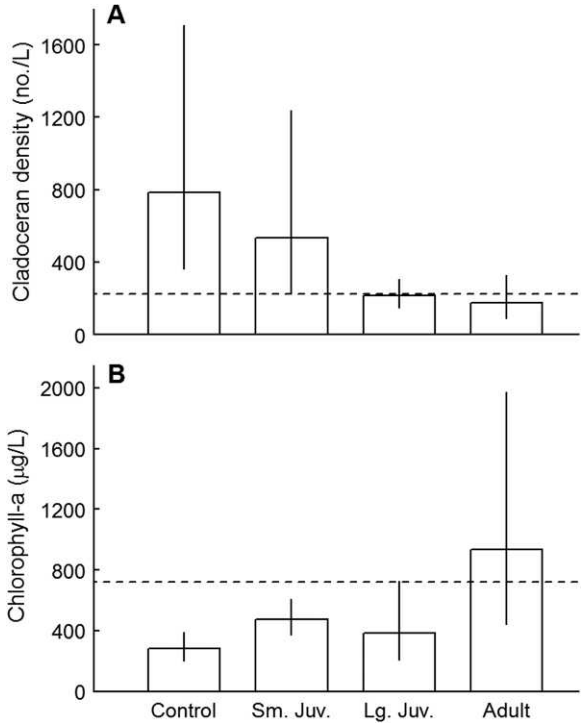

Fig. 3. Influence of *Trichocorixa* presence and life-history stage on the density of (A) cladocerans (*Moina* and *Daphnia* combined) and (B) phytoplankton (measured as chlorophyll-*a*) after 12 days in the mesocosm experiment. Data are back-transformed means ± SD; N = 4 for each treatment level. The dashed horizontal lines represent the density of each trophic level just prior to *Trichocorixa* addition (A: 223 cladocerans/L; B: 719 μg chlorophyll-*a*/L). Treatment levels are represented along the *x*-axis: Control (no *Trichocorixa*), Small Juveniles (second and third instars), Large Juveniles (fourth and fifth instars), and Adults.

phytoplankton, 0.58 for *Moina*, and 0.37 for *Trichocorixa* (using a 0-time lag and averaging the three possible pairwise cross-correlation coefficients for each trophic level).

The MARSS model fit indicated that top-down interactions were the only trophic factors influencing population dynamics in the field: the *Trichocorixa*→*Moina* (−0.16) and *Moina*→phytoplankton (−0.06) terms were the only non-autoregressive interaction strengths remaining in the best-fit model (Table 3). Because these two direct interactions were both significantly negative, and not countered by a negative *Trichocorixa*→phytoplankton term, the model indicates that increases in *Trichocorixa* biomass led to decreases in *Moina* density, which led to increases in phytoplankton chlorophyll-*a*. That is, according to the MARSS model, the trophic cascade was detectible in the time-series data. Indeed, if the *Trichocorixa*→*Moina* and *Moina*→phytoplankton terms were excluded from the model, the *Trichocorixa*→phytoplankton interaction became significantly positive (maximum likelihood estimate: 0.08, 95% CI: 0.0–0.15). That the *Trichocorixa*→phytoplankton term was not retained in the best-fit model, however, suggests that the trophic cascade was approximated well by the linear combination of the two direct top-down effects. None of the bottom-up terms were retained in the best-fit model, but temperature did positively affect all three trophic level's rates of increase (Table 3; Fig. 4D). Temperature was also strongly correlated among pools (average of the three between-pool cross-correlation coefficients was 0.97), and therefore likely contributed to the temporal dynamics of all three trophic levels being synchronized across the three pools (Figs. 4, 5). Salinity, however, did not influence any trophic level in the pools, likely because salt concentrations remained low during the entire survey (see Appendix B: Fig. B3 for all non-temperature environmental data).

Discussion

Here I have combined laboratory and field experiments with field survey data in a freshwater ecosystem to highlight the role that ontogenetic changes in top predator consumption rates play in structuring food webs. Similar to many other predator taxa, *Trichocorixa* grew substantially during its life history, with concomitant increases in consumption rates (Peters 1983, Kooijman 1993). The allometric increase in per capita consumption by *Trichocorixa* manifested in the rock-pool food web as an increase in top-down control with predator ontogeny, as demonstrated experimentally and observed in field data. Similar to other field populations of *Trichocorixa* (Tones 1977, Kelts 1979), the populations surveyed here showed a non-stable stage structure with partially overlapping generations and a fluctuating total population size (Appendix B: Fig. B2), which led to a dynamic *Trichocorixa* biomass (and predation rate) and caused the

21508925, 2013, 5, Downloaded from https://esajournals.onlinelibrary.wiley.com/doi/10.1890/ES13-00019.1, Wiley Online Library on [22/01/2026]. See the Terms and Conditions (https://onlinelibrary.wiley.com/terms-and-conditions) on Wiley Online Library for rules of use; OA articles are governed by the applicable Creative Commons License

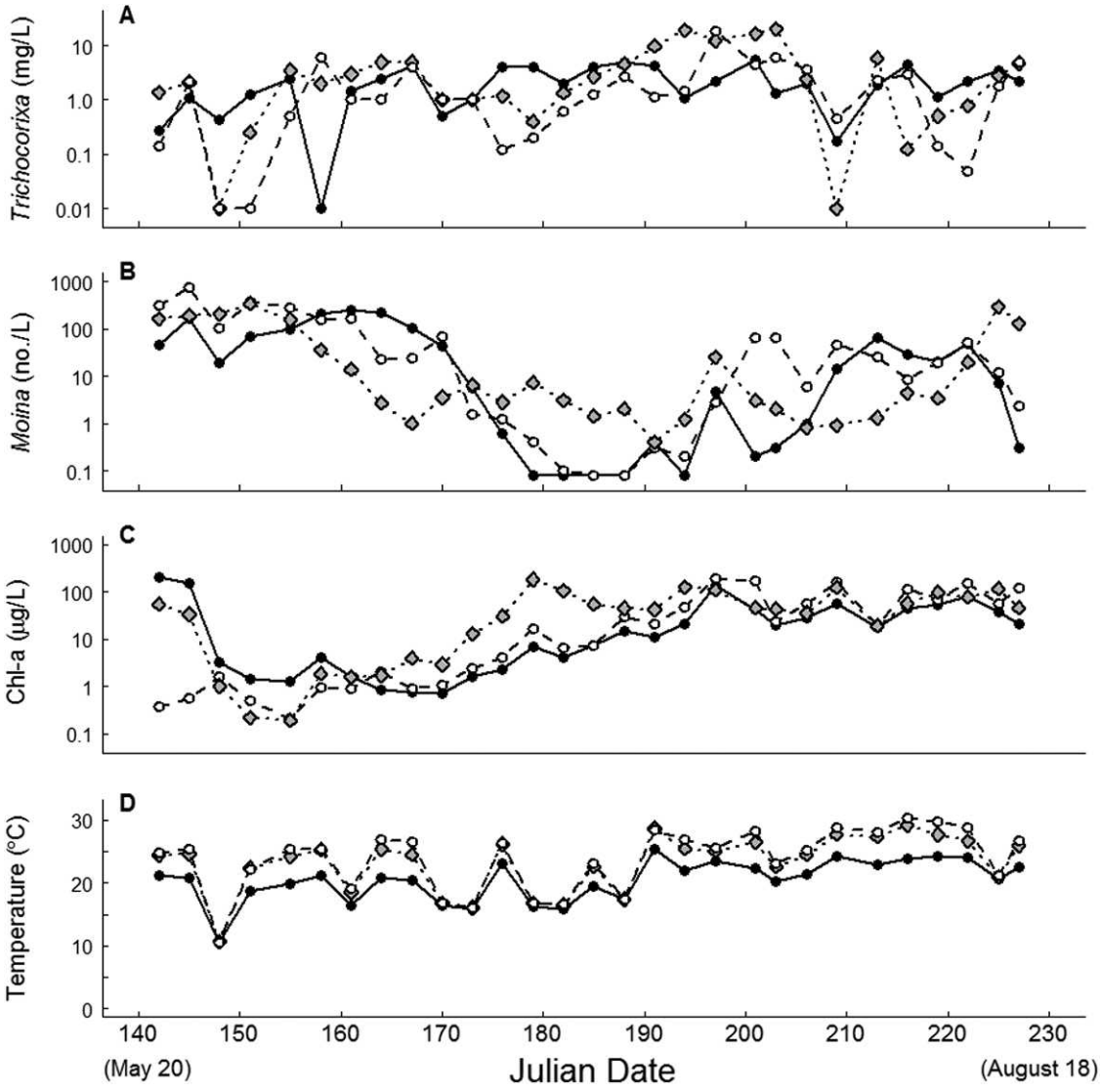

Fig. 4. Time series of (A) *Trichocorixa*, (B) *Moina*, and (C) phytoplankton densities and temperature (D) in three rock pools during the summer of 2009. Each set of point and line types represents a different pool and are consistent across panels. Note the $\log_{10}$ scales of the *y*-axes in (A, B, C) and the difference in range for the *y*-axis in (A) compared to (B and C). For additional physicochemical data, see Appendix B: Fig. B3.

direct and indirect effects of *Trichocorixa* predation to vary through time. This type of demographically driven variation in predation strength may be common given the prevalence of both allometrically scaling consumption rates and dynamically structured predator populations (Peters 1983, Ebenman and Persson 1988, Werner 1988, Kooijman 1993), and indicates that the inclusion of stage- or size-specific information may be important for understanding the trophic structure and dynamics of food webs (Alford 1989, Hairston and Hairston 1997, de Roos et al. 2003).

The degree to which top predator ontogeny influences trophic dynamics is likely mediated by other ecological factors, such as the complexity of the particular food web (Hairston and Hairston 1997, Hildrew et al. 2007*b*). Changes in top predator consumption rates are far more likely to have straightforward cascading effects in a

21508925, 2013, 5, Downloaded from https://esajournals.onlinelibrary.wiley.com/doi/10.1890/ES13-00019.1, Wiley Online Library on [22/01/2026]. See the Terms and Conditions (https://onlinelibrary.wiley.com/terms-and-conditions) on Wiley Online Library for rules of use; OA articles are governed by the applicable Creative Commons License

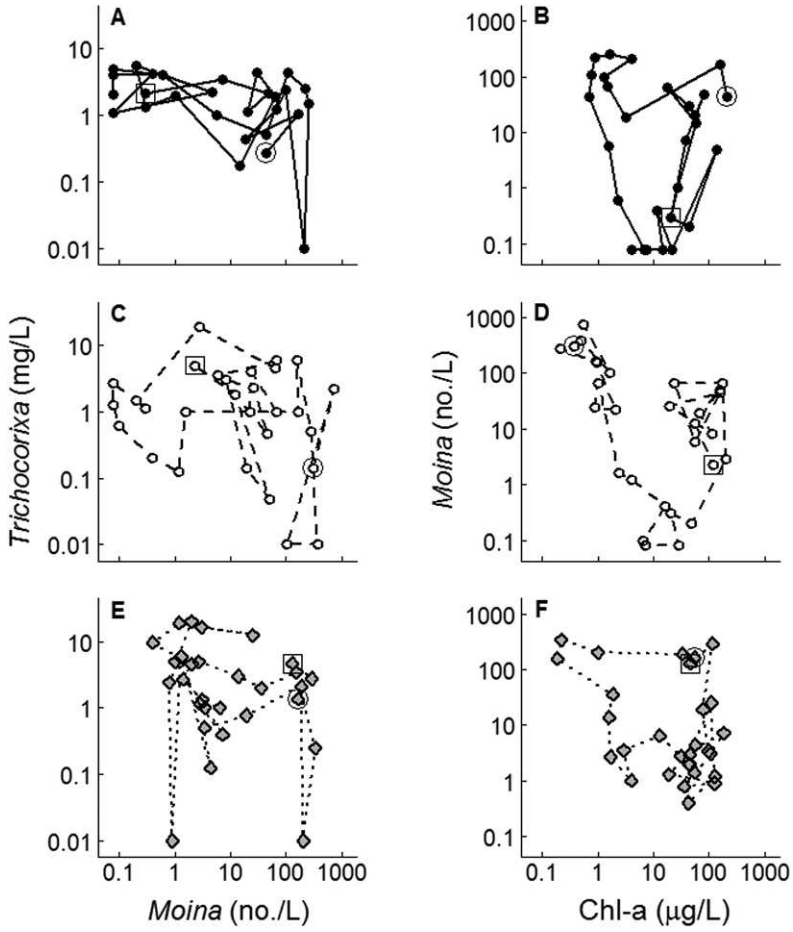

Fig. 5. Phase planes depicting the relationship between *Trichocorixa* biomass and *Moina* density (A, C, E) and the relationship between *Moina* density and phytoplankton chlorophyll-*a* (B, D, F) in each of the three pools shown in Fig. 4 (point and line types match those in Fig. 4). The circled point is the beginning of the time series and the boxed point is the end of the time series.

simple tri-trophic food chain like the (dominant) chain in the Appledore rock pools than they are in a more complex food web with many constituents and linkages. Indeed, *Trichocorixa* is capable of consuming a wider variety of resources than what is present and accessible in the rock pools (e.g., filamentous algae, dipteran larvae; Kelts 1979). The higher food-web complexity found in other ecosystems *Trichocorixa* inhabits could alter the trophic influence of this species, and its ontogeny, on food-web structure and dynamics (Polis and Strong 1996, Hairston and Hairston 1997). For example, the presence of alternative resource types that supplement the diet of young *Trichocorixa* instars could help meet the high energetic demands of these stages, thereby reducing mortality rates, but may also induce an ontogenetic niche shift.

In addition to food-web complexity, population structure within other trophic levels may also modulate the trophic effect of ontogenetic changes in the top predator. For example, many species at lower trophic levels also grow considerably over their lifetimes, which likely has consequences for their trophic interactions as both resources and consumers. This is the case in the Appledore pools, as both *Moina* and *Daphnia* grow considerably during their own ontogeny (Anderson et al. 1937, Martínez-Jerónimo and Gutierrez-Valdivia 1991), which likely influences both their vulnerability to predators and their grazing rates (Murdoch and Scott 1984, Knoechel

21508925, 2013, 5, Downloaded from https://esajournals.onlinelibrary.wiley.com/doi/10.1890/ES13-00019.1, Wiley Online Library on [22/01/2026]. See the Terms and Conditions (https://onlinelibrary.wiley.com/terms-and-conditions) on Wiley Online Library for rules of use; OA articles are governed by the applicable Creative Commons License

Table 3. Parameter estimates and approximate 95% CIs for the best-fitting MARSS model fit to the field survey data.

Parameter	Phytoplankton	*Moina*	*Trichocorixa*	Temperature
Phytoplankton	0.88 [0.83 to 0.93]	−0.06 [−0.09 to −0.04]		0.05 [0.02 to 0.07]
Moina		0.92 [0.87 to 0.96]	−0.16 [−0.30 to −0.02]	0.05 [0.01 to 0.09]
Trichocorixa			0.62 [0.41 to 0.84]	0.05 [−0.01 to 0.10]

Notes: The MARSS model was fit using maximum likelihood estimation and the best model was chosen based on AICc scores. Parameters are shown as the effect of the column at time $t - 1$ on the row at time t. Empty entries correspond to (non-significant) parameters that were removed from the model. No salinity effects were in the final model, so it is absent from the table. Confidence intervals are shown in the brackets and were approximated from the Hessian matrix using the MARSSparamCIs function in the MARSS R package (Holmes et al. 2012). Units are: phytoplankton in log(μg chl-*a*/L), *Moina* in log(no./L), *Trichocorixa* in log(mg dry mass/L), and temperature in °C.

and Holtby 1986). Although it is currently unknown how selective or efficient *Trichocorixa* is when preying upon cladocerans of different sizes within the same species, many other predatory aquatic insects show strong selection for, and higher predation rates on, smaller prey size classes (e.g., Thompson 1975, Pastorok 1981, Murdoch and Scott 1984, Ranta and Espo 1989). Indeed, *Trichocorixa* is negatively size-selective when preying upon *Artemia* brine shrimp (Wurtsbaugh 1992), which corresponds to the preference for the smaller cladoceran species (*Moina* over *Daphnia*) shown in the present study (Fig. 2) and suggests a general preference for smaller prey items. Considering that the rates at which cladocerans graze on phytoplankton is also strongly size-dependent (Knoechel and Holtby 1986, Kooijman 1993, DeMott et al. 2010), selection by *Trichocorixa* for specific size-classes of cladocerans may have cascading effects on phytoplankton densities and dynamics. Such size-specific interactions have the potential to alter the dynamics of tri-trophic food webs qualitatively by introducing Allee effects or stabilizing population cycles (de Roos et al. 2003). It is therefore likely that the complete picture of the food-web consequences caused by ontogenetically variable predators such as *Trichocorixa* results from a combination of predator and prey population size structures.

Despite potential confounding factors such as prey size distributions, increases in *Trichocorixa* biomass (and predation rate) did cause significant reductions in *Moina* population growth rates in situ (Figs. 4, 5). The observed trophic dynamics were similar across pools and were consistent with expectation based on the experimental results (Fig. 3). In particular, *Moina* densities decreased with the increase in *Trichocorixa* biomass resulting from the first generation maturing through the last juvenile stages and into adulthood, then remained low until after *Trichocorixa* biomass decreased when the second generation crashed. That is, the relevant changes in *Trichocorixa* biomass and predation rate were the result of a combination of ontogenetic growth, reproduction, and mortality. The strong reduction in prey densities that resulted from the period of high *Trichocorixa* biomass had important consequences for both the *Trichocorixa* populations and the rest of the rock-pool food web. After reducing *Moina* to near-extinction, the adult *Trichocorixa* densities decreased (Fig. B2), perhaps driven by flighted emigration in response to low resource densities, an expectation for motile predators based on optimal foraging theory (Charnov 1976) which occurs in this system (adult *Trichocorixa* emigration rates are negatively related to *Moina* densities; Simonis 2012). The reduced predation that resulted from the decrease in adults may have contributed to the persistence of the *Moina* populations in the pools, despite their reaching very low densities, and would therefore point to the role of predator dispersal in stabilizing locally unstable food webs at larger spatial scales (Murdoch and Stewart-Oaten 1989, Simonis 2012).

The period of low *Moina* densities may have also contributed to the mass mortality seen in the early instars of the second *Trichocorixa* generation (ca. Julian Day 200; Figs. 4, 5), as these young stages have high energetic demands (see daily specific consumption in Table 2) that may not have been met by the low densities of prey present when they hatched. Cannibalism by adults, which is widespread among the Corixidae (Pajunen and Pajunen 1991), may also have contributed to the high mortality experienced by

21508925, 2013, 5, Downloaded from https://esajournals.onlinelibrary.wiley.com/doi/10.1890/ES13-00019.1, Wiley Online Library on [22/01/2026]. See the Terms and Conditions (https://onlinelibrary.wiley.com/terms-and-conditions) on Wiley Online Library for rules of use; OA articles are governed by the applicable Creative Commons License

juvenile *Trichocorixa* in the field. However, there is no published information regarding cannibalism in *Trichocorixa* and I have not observed it in any of my studies on this species, which included experiments designed to test specifically for cannibalism (J. L. Simonis, *unpublished data*). Further, the density of adults (the most likely cannibalistic stage; Pajunen and Pajunen 1991) in the pools was very low during the time when the second generation crashed (Appendix B: Fig. B2). Whatever its cause, the high juvenile mortality resulted in generally low recruitment of the second *Trichocorixa* generation in these populations (Fig. 4A; Appendix B: Fig. B2), which could promote longer term persistence of local *Moina* populations. Indeed, the *Moina* populations did eventually recover in all three pools, but not until later in the season, after the *Trichocorixa* biomass decreased due to the high mortality of the second generation (Figs. 4, 5; Appendix B: Fig. B2).

Ontogenetic shifts in feeding ecology, such as those shown here for *Trichocorixa*, are widespread among animal taxa and can strongly influence the structure and dynamics of food webs (Peters 1983, Werner and Gilliam 1984, Werner 1988, Polis and Strong 1996, Persson et al. 1998, Rudolf and Lafferty 2011). Although most research has focused on the food-web effects of qualitative feeding shifts, many predators exhibit less extreme, but still important, quantitative changes in feeding rates with ontogeny (Peters 1983, Kooijman 1993). Here I have shown that an ontogenetic allometric increase in the per capita rate of predation by *Trichocorixa verticalis* on cladoceran zooplankton strengthened the trophic cascade to primary producers in freshwater rock pools. As a result, predation by adult *Trichocorixa* led to much stronger top-down control than did predation by juvenile *Trichocorixa*. Just as among-taxa differences in predation rates and efficiencies may dictate the presence or strength of trophic cascades across ecosystems (Hairston and Hairston 1993, Polis 1999, Borer et al. 2005), ontogenetic variation in predation rates within top predator taxa may influence trophic dynamics within ecosystems. As a result, the size-structure of predator populations may play an important role in dictating when or how strongly trophic cascades will appear within a particular ecosystem. These results indicate that quantitative ontogenetic changes in predator feeding may also have significant food-web consequences, and suggest that merging population and food web ecology may be necessary to understand and predict field ecosystem dynamics more accurately (Alford 1989, Hairston and Hairston 1993, de Roos et al. 2003, Cohen et al. 2003, Hildrew et al. 2007*a*).

Acknowledgments

Many thanks to the staff of the Shoals Marine Laboratory (SML) for logistical assistance, in particular to SML director W. Bemis. Thanks also to J. Morin and E. Kuo for preliminary research on the rock-pool system and to the Hairston and Flecker groups for earlier discussions on this topic. This manuscript was improved by the comments of A. Agrawal, S. Ellner, A. Flecker, M. Booth, K. Capps, N. Hairston Jr., S. Simonis, and four anonymous reviewers. I. Hewson, L. Quevillon, and P. Thompson provided field assistance. This work was supported financially by the Shoals Marine Laboratory, Cornell University Biogeochemistry and Environmental Biocomplexity Program, and a National Science Foundation Graduate Research Fellowship awarded to JLS. This is contribution #165 from the Shoals Marine Laboratory.

Literature Cited

Abramoff, M. D., P. J. Magelhaes, and S. J. Ram. 2004. Image processing with ImageJ. Biophotonic International 11:36–42.

Alford, R. A. 1989. Variation in predator phenology affects predator performance and prey community composition. Ecology 70:206–219.

Aljetlawi, A. A., E. Sparrevik, and K. Leonardsson. 2004. Prey-predator size-dependent functional response: derivation and rescaling to the real world. Journal of Animal Ecology 73:239–252.

Anderson, B. G., H. Lumer, and L. J. Zupancic, Jr. 1937. Growth and variability in *Daphnia pulex*. Biological Bulletin 73:444–463.

Bolker, B. and R Development Core Team. 2011. bbmle: tools for general maximum likelihood estimation. R package version 0.9.7. http://CRAN.R-project.org/package=bbmle

Borer, E. T., E. W. Seabloom, J. B. Shurin, K. E. Anderson, C. A. Blanchette, B. Broitman, S. D. Cooper, and B. S. Halpern. 2005. What determines the strength of a trophic cascade? Ecology 86:528–537.

Brown, J. H., J. F. Gillooly, A. P. Allen, V. M. Savage, and G. B. West. 2004. Towards a metabolic theory of ecology. Ecology 85:1771–1789.

Byström, P. and J. Andersson. 2005. Size-dependent foraging capacities and intercohort competition in

21508925, 2013, 5, Downloaded from https://esajournals.onlinelibrary.wiley.com/doi/10.1890/ES13-00019.1, Wiley Online Library on [22/01/2026]. See the Terms and Conditions (https://onlinelibrary.wiley.com/terms-and-conditions) on Wiley Online Library for rules of use; OA articles are governed by the applicable Creative Commons License

an ontogenetic omnivore (Arctic char). Oikos 110:523–536.

Carpenter, S. R., K. L. Cottingham, and C. A. Stow. 1994. Fitting predator-prey models to time series with observation errors. Ecology 75:1254–1264.

Charnov, E. L. 1976. Optimal foraging, the Marginal Value Theorem. Theoretical Population Biology 9:129–136.

Chesson, J. 1978. Measuring preference in selective predation. Ecology 59:211–215.

Chesson, J. 1983. The estimation and analysis of preference and its relationship to foraging models. Ecology 64:1297–1304.

Cohen, J. E., T. Jonsson, and S. R. Carpenter. 2003. Ecological community description using the food web, species abundance, and body size. Proceedings of the National Academy of Sciences 100:1781–1786.

de Roos, A. M., J. A. J. Metz, E. Evers, and A. Leipoldt. 1990. A size dependent predator-prey interaction: who pursues whom? Journal of Mathematical Biology 28:609–643.

de Roos, A. M. and L. Persson. 2002. Size-dependent life-history traits promote catastrophic collapses of top predators. Proceedings of the National Academy of Sciences 99:12907–12912.

de Roos, A. M., L. Persson, and E. McCauley. 2003. The influence of size-dependent life-history traits on the structure and dynamics of populations and communities. Ecology Letters 6:473–487.

DeMott, W. R., E. N. McKinney, and A. J. Tessier. 2010. Ontogeny of digestion in *Daphnia*: implications for the effectiveness of algal defenses. Ecology 91:540–548.

Dillon, P. M. 1985. Chironomid larval size and case presence influence capture success achieved by dragonfly larvae. Freshwater Invertebrate Biology 4:22–29.

Ebenman, B. and L. Persson. 1988. Size-structured populations: ecology and evolution. Springer-Verlag, Berlin, Germany.

Gotelli, N. J. and A. M. Ellison. 2004. A primer of ecological statistics. Sinauer Associates, Sunderland, Massachusetts, USA.

Hairston, N. G., F. E. Smith, and L. B. Slobodkin. 1960. Community structure, population control, and competition. American Naturalist 94:421–425.

Hairston, N. G., Jr. and N. G. Hairston, Sr. 1993. Cause-effect relationships in energy flow, trophic structure, and interspecific interactions. American Naturalist 142:379–411.

Hairston, N. G., Jr. and N. G. Hairston, Sr. 1997. Does food web complexity eliminate trophic-level dynamics? American Naturalist 149:1001–1007.

Hambright, K. D., N. G. Hairston, Jr., W. R. Schaffner, and R. W. Howarth. 2007. Grazer control of nitrogen fixation: phytoplankton taxonomic composition and ecosystem functioning. Fundamental and Applied Limnology 170:103–124.

Hildrew, A., D. Raffaelli, and R. Edmonds-Brown. 2007*a*. Body size: the structure and function of aquatic ecosystems. Cambridge University Press, Cambridge, UK.

Hildrew, A., D. Raffaelli, and R. Edmonds-Brown. 2007*b*. Body size in aquatic ecology: important, but not the whole story. Pages 326–334 *in* A. Hildrew, D. Raffaelli, and R. Edmonds-Brown, editors. Body size: the structure and function of aquatic ecosystems. Cambridge University Press, Cambridge, UK.

Holmes, E. E. 2012. Derivation of the EM algorithm for constrained and unconstrained mars models. Technical report. Northwest Fisheries Science Center, Mathematical Biology Program.

Holmes, E. E., E. J. Ward, and K. Wills. 2012. Marss: Multivariate autoregressive state-space models for analyzing time-series data. The R Journal 4:11–19.

Ives, A. R., S. R. Carpenter, and B. Dennis. 1999. Community interaction webs and zooplankton responses to planktivory manipulations. Ecology 80:1405–1421.

Ives, A. R., B. Dennis, K. L. Cottingham, and S. R. Carpenter. 2003. Estimating community stability and ecological interactions from time-series data. Ecological Monographs 73:301–330.

Jansson, A. 1982. Notes on some Corixidae (Heteroptera) from New Guinea and New Caledonia. Pacific Insects 24:95–103.

Jones, J. I. and E. Jeppesen. 2007. Body size and trophic cascades in lakes. Pages 118–139 *in* A. Hildrew, D. Raffaelli, and R. Edmonds-Brown, editors. Body size: the structure and function of aquatic ecosystems. Cambridge University Press, Cambridge, UK.

Kelts, L. J. 1979. Ecology of a tidal marsh corixid, *Trichocorixa verticalis* (Insecta, Hemiptera). Hydrobiologia 64:37–57.

Knoechel, R. and L. B. Holtby. 1986. Cladoceran feeding rate: body length relationships for bacterial and large algal particles. Limnology and Oceanography 31:195–200.

Kooijman, S. A. L. M. 1993. Dynamical energy budgets in biological systems. Cambridge University Press, Cambridge, UK.

Loder, T. C., III, B. Ganning, and J. A. Love. 1996. Ammonia nitrogen dynamics in coastal rockpools affected by gull guano. Journal of Experimental Marine Biology and Ecology 196:113–129.

Manly, B. F. J. 1974. A model for certain types of selection experiments. Biometrics 30:281–294.

Martínez-Jerónimo, F. and A. Gutierrez-Valdivia. 1991. Fecundity, reproduction, and growth of *Moina macrocopa* fed different algae. Hydrobiologia 222:49–55.

21508925, 2013, 5, Downloaded from https://esajournals.onlinelibrary.wiley.com/doi/10.1890/ES13-00019.1, Wiley Online Library on [22/01/2026]. See the Terms and Conditions (https://onlinelibrary.wiley.com/terms-and-conditions) on Wiley Online Library for rules of use; OA articles are governed by the applicable Creative Commons License

Mittelbach, G. G. 1981. Foraging efficiency and body size: a study of optimal diet and habitat use by bluegills. Ecology 65:1370–1386.

McCauley, E. 1984. The estimation of the abundance and biomass of zooplankton in samples. Pages 228–263 *in* J. A. Downing and F. H. Rigler, editors. A manual on methods for the assessment of secondary productivity in fresh waters. Second edition. Blackwell Scientific, Oxford, UK.

McCoy, M. W. and B. M. Bolker. 2008. Trait-mediated interactions: influence of prey size, density, and experience. Journal of Animal Ecology 77:478–486.

Murdoch, W. M. and M. A. Scott. 1984. Stability and extinction of laboratory populations of zooplankton preyed on by the backswimmer *Notonecta*. Ecology 65:1231–1248.

Murdoch, W. M. and A. Stewart-Oaten. 1989. Aggregation by parasitoids and predators: effects on equilibrium and stability. American Naturalist 134:288–310.

Nandini, S. and S. S. S. Sarma. 2000. Lifetable demography of four cladoceran species in relation to algal food (*Chlorella vulgaris*) density. Hydrobiologia 435:117–126.

Nusch, E. A. 1980. Comparison of different methods for chlorophyll and phaeopigment determination. Archiv fur Hydrobiologia 14:14–36.

Pace, M. L., J. J. Cole, S. R. Carpenter, and J. F. Kitchell. 1999. Trophic cascades revealed in diverse ecosystems. Trends in Ecology and Evolution 14:483–488.

Paine, R. T. 1980. Food webs: linkage, interaction strength, and community infrastructure. Journal of Animal Ecology 49:666–685.

Pajunen, V. I. and I. Pajunen. 1991. Oviposition and egg cannibalism in rock-pool Corixids (Hemiptera: Corixidae). Oikos 60:83–90.

Pajunen, V. I. and I. Pajunen. 2007. Habitat characteristics contributing to local occupancy and habitat use in rock pool Daphnia metapopulations. Hydrobiologia 592:291–302.

Pastorok, R. A. 1981. Prey vulnerability and size selection by *Chaoborus* larvae. Ecology 62:1311–1324.

Persson, L. 1987. The effects of resource availability and distribution on size class interactions in perch, *Perca fluviatilis*. Oikos 48:148–160.

Persson, L., K. Leonardsson, A. M. de Roos, M. Gyllenber, and B. Christensen. 1998. Ontogenetic scaling of foraging rates and the dynamics of a size-structured consumer-resource model. Theoretical Population Biology 54:270–293.

Peters, R. H. 1983. The ecological implications of body size. Cambridge University Press, Cambridge, UK.

Polis, G. A. and D. R. Strong. 1996. Food web complexity and community dynamics. American Naturalist 147:813–846.

Polis, G. A. 1999. Why are parts of the world green? Multiple factors control productivity and the distribution of biomass. Oikos 86:3–15.

R Development Core Team. 2011. R: a language and environment for statistical computing. R Foundation for Statistical Computing, Vienna, Austria.

Ranta, E. and J. Espo. 1989. Predation by the rock-pool insects *Arctocorisa carinata*, *Callieorixa producta* (Het. Corixidae) and *Potamonectes griseostriatus* (Col. Dytiscidae). Annales Zoologici Fennici 26:53–60.

Rogers, D. J. 1972. Random search and insect population models. Journal of Animal Ecology 41:369–383.

Rudolf, V. H. W. 2007. The interaction of cannibalism and omnivory: consequences for community dynamics. Ecology 88:2697–2705.

Rudolf, V. H. W. and K. D. Lafferty. 2011. Stage structure alters how complexity affects stability of ecological networks. Ecology Letters 14:75–79.

Sala, J. and D. Boix. 2005. Presence of the Nearctic water boatman *Trichocorixa verticalis verticalis* (Fieber, 1851) (Heteroptera, Corixidae) in the Algarve region (S Portugal). Graellsia 61:31–36.

Schmitz, O. J., P. A. Hambäck, and A. P. Beckerman. 2000. Trophic cascades in terrestrial systems: a review of the effects of carnivore removal on plants. American Naturalist 155:141–153.

Shine, R. 1991. Why do larger snakes eat larger prey items? Functional Ecology 5:493–502.

Shurin, J. B., E. T. Borer, E. W. Seabloom, K. Anderson, C. A. Blanchette, B. Broitman, S. D. Cooper, and B. S. Halpern. 2002. A cross-ecosystem comparison of the strength of trophic cascades. Ecology Letters 5:785–791.

Simonis, J. L. 2012. Prey (*Moina macrocopa*) population density drives emigration rate of its predator (*Trichocorixa verticalis*) in a rock-pool metacommunity. Hydrobiologia. doi: 10.1007/s10750-012-1268-9

Strong, D. R. 1992. Are all trophic cascades wet? Differentiation and donor-control in speciose ecosystems. Ecology 73:747–754.

Sze, P. 1981. Observations on microalgae in supralittoral rockpools in New England (USA). Botanica Marina 24:337–341.

Thompson, D. J. 1975. Towards a predator-prey model incorporating age structure: the effects of predator and prey size on the predation of *Daphnia magna* by *Ischnura elegans*. Journal of Animal Ecology 44:907–916.

Tones, P. I. and U. T. Hammer. 1975. Osmoregulation in *Trichocorixa verticalis interiores* Sailer (Hemiptera, Corixidae)—an inhabitant of Saskatchewan saline lakes, Canada. Canadian Journal of Zoology 53:1207–1212.

Tones, P. I. 1977. The life cycle of *Trichocorixa verticalis interiors* Sailer (Hempitera, Corixidae) with special reference to diapause. Freshwater Biology 7:31–36.

van de Meutter, F., H. Trekels, and A. J. Green. 2010.

21508925, 2013, 5, Downloaded from https://esajournals.onlinelibrary.wiley.com/doi/10.1890/ES13-00019.1, Wiley Online Library on [22/01/2026]. See the Terms and Conditions (https://onlinelibrary.wiley.com/terms-and-conditions) on Wiley Online Library for rules of use; OA articles are governed by the applicable Creative Commons License

The impact of the North American waterbug *Trichocorixa verticalis* (Fieber) on aquatic macroinvertebrate communities in southern Europe. Fundamental and Applied Limnology 177:283–292.
Werner, E. E. and J. F. Gilliam. 1984. The ontogenetic niche and species interactions in size-structured populations. Annual Review of Ecology and Systematics 15:393–425.
Werner, E. E. 1988. Size, scaling, and the evolution of complex life cycles. Pages 60–81 *in* B. Ebenman and L. Persson, editors. Size-structured populations: ecology and evolution. Springer-Verlag, Berlin, Germany.
Wetzel, R. G. and G. E. Likens. 2000. Limnological analyses. Third edition. Springer, Berlin, Germany.
Woodward, G. and A. G. Hildrew. 2002. Body-size determinants of niche overlap and intraguild predation within a complex food web. Journal of Animal Ecology 71:1063–1074.
Wurtsbaugh, W. A. and T. S. Berry. 1990. Cascading effects of decreased salinity on the plankton, chemistry, and physics of the Great Salt Lake (Utah). Canadian Journal of Fisheries and Aquatic Sciences 47:100–109.
Wurtsbaugh, W. A. 1992. Food-web modification by an invertebrate predator in the Great Salt Lake (USA). Oecologia 89:168–175.

Supplemental Material

Appendix A

In the main text, the MARSS model was shown in compact matrix notation (Eq. 2). In this appendix, I give the model in its full form. I also explain the interpolation-extrapolation procedure used for the covariate data.

MARSS model articulation

In the main text (as Eq. 2), the MARSS model was shown in compact form

$$\mathbf{x}_t = \mathbf{B}\mathbf{x}_{t-1} + \mathbf{u} + \mathbf{C}\mathbf{c}_t + \mathbf{w}_t \quad \text{where } \mathbf{w}_t \sim \text{MVN}(0, \mathbf{Q}) \tag{A1a}$$

$$\mathbf{y}_t = \mathbf{x}_t + \mathbf{v}_t \quad \text{where } \mathbf{v}_t \sim \text{MVN}(0, \mathbf{R}) \tag{A1b}$$

where, for example, $\mathbf{x}_t$ is actually a 9×1 matrix, with a row for each trophic level in each of the three pools. Within each pool, the model is structured as

$$\begin{bmatrix} x_p \\ x_M \\ x_T \end{bmatrix}_t = \begin{bmatrix} b_{p\to p} & b_{M\to p} & b_{T\to p} \\ b_{p\to M} & b_{M\to M} & b_{T\to M} \\ b_{p\to T} & b_{M\to T} & b_{T\to T} \end{bmatrix} \begin{bmatrix} x_p \\ x_M \\ x_T \end{bmatrix}_{t-1} + \begin{bmatrix} u_p \\ u_M \\ u_T \end{bmatrix} + \begin{bmatrix} c_{te\to p} & c_{sa\to p} \\ c_{te\to M} & c_{sa\to M} \\ c_{te\to T} & c_{sa\to T} \end{bmatrix} \begin{bmatrix} te \\ sa \end{bmatrix}_t + \begin{bmatrix} w_p \\ w_M \\ w_T \end{bmatrix}_t$$

$$\text{where } \begin{bmatrix} w_p \\ w_M \\ w_T \end{bmatrix}_t = \text{MVN}\left(0, \begin{bmatrix} q_p & 0 & 0 \\ 0 & q_M & 0 \\ 0 & 0 & q_T \end{bmatrix}\right) \tag{A2a}$$

for the state-process model and

$$\begin{bmatrix} y_p \\ y_M \\ y_T \end{bmatrix}_t = \begin{bmatrix} x_p \\ x_M \\ x_T \end{bmatrix}_t + \begin{bmatrix} v_p \\ v_M \\ v_T \end{bmatrix}_t \text{ where } \begin{bmatrix} v_p \\ v_M \\ v_T \end{bmatrix}_t = \text{MVN}\left(0, \begin{bmatrix} 0.007 & 0 & 0 \\ 0 & 0.10 & 0 \\ 0 & 0 & 0.30 \end{bmatrix}\right) \tag{A2b}$$

for the observation-process model. Here, *p*, *M*, *T*, *te*, and *sa* refer to phytoplankton, *Moina*, *Trichocorixa*, temperature, and salinity (respectively) and the arrows in subscripts reflect the directionality of the effect (e.g., $p \to M$ refers to the effect of phytoplankton on *Moina*). As explained in the main text, the variances describing the observation errors ($\mathbf{v}_t$) were estimated independently and fixed. That the off-diagonal entries in $\mathbf{Q}$ and $\mathbf{R}$ are all 0 reflects the assumption that there is no covariance in either the process or observation errors among trophic levels.

When all three pools are included, the model expands to its full form:

21508925, 2013, 5, Downloaded from https://esajournals.onlinelibrary.wiley.com/doi/10.1890/ES13-00019.1, Wiley Online Library on [22/01/2026]. See the Terms and Conditions (https://onlinelibrary.wiley.com/terms-and-conditions) on Wiley Online Library for rules of use; OA articles are governed by the applicable Creative Commons License

$$\begin{bmatrix} x_{p1} \\ x_{M1} \\ x_{T1} \\ x_{p2} \\ x_{M2} \\ x_{T2} \\ x_{p3} \\ x_{M3} \\ x_{T3} \end{bmatrix}_t = \begin{bmatrix} b_{p\to p} & b_{M\to p} & b_{T\to p} & 0 & 0 & 0 & 0 & 0 & 0 \\ b_{p\to M} & b_{M\to M} & b_{T\to M} & 0 & 0 & 0 & 0 & 0 & 0 \\ b_{p\to T} & b_{M\to T} & b_{T\to T} & 0 & 0 & 0 & 0 & 0 & 0 \\ 0 & 0 & 0 & b_{p\to p} & b_{M\to p} & b_{T\to p} & 0 & 0 & 0 \\ 0 & 0 & 0 & b_{p\to M} & b_{M\to M} & b_{T\to M} & 0 & 0 & 0 \\ 0 & 0 & 0 & b_{p\to T} & b_{M\to T} & b_{T\to T} & 0 & 0 & 0 \\ 0 & 0 & 0 & 0 & 0 & 0 & b_{p\to p} & b_{M\to p} & b_{T\to p} \\ 0 & 0 & 0 & 0 & 0 & 0 & b_{p\to M} & b_{M\to M} & b_{T\to M} \\ 0 & 0 & 0 & 0 & 0 & 0 & b_{p\to T} & b_{M\to T} & b_{T\to T} \end{bmatrix} \begin{bmatrix} x_{p1} \\ x_{M1} \\ x_{T1} \\ x_{p2} \\ x_{M2} \\ x_{T2} \\ x_{p3} \\ x_{M3} \\ x_{T3} \end{bmatrix}_{t-1}$$

$$+ \begin{bmatrix} u_{p1} \\ u_{M1} \\ u_{T1} \\ u_{p2} \\ u_{M2} \\ u_{T2} \\ u_{p3} \\ u_{M3} \\ u_{T3} \end{bmatrix} + \begin{bmatrix} c_{te\to p} & c_{sa\to p} & 0 & 0 & 0 & 0 \\ c_{te\to M} & c_{sa\to M} & 0 & 0 & 0 & 0 \\ c_{te\to T} & c_{sa\to T} & 0 & 0 & 0 & 0 \\ 0 & 0 & c_{te\to p} & c_{sa\to p} & 0 & 0 \\ 0 & 0 & c_{te\to M} & c_{sa\to M} & 0 & 0 \\ 0 & 0 & c_{te\to T} & c_{sa\to T} & 0 & 0 \\ 0 & 0 & 0 & 0 & c_{te\to p} & c_{sa\to p} \\ 0 & 0 & 0 & 0 & c_{te\to M} & c_{sa\to M} \\ 0 & 0 & 0 & 0 & c_{te\to T} & c_{sa\to T} \end{bmatrix} \begin{bmatrix} te_1 \\ sa_1 \\ te_2 \\ sa_2 \\ te_3 \\ sa_3 \end{bmatrix}_t + \begin{bmatrix} w_{p1} \\ w_{M1} \\ w_{T1} \\ w_{p2} \\ w_{M2} \\ w_{T2} \\ w_{p3} \\ w_{M3} \\ w_{T3} \end{bmatrix}_t$$

$$\text{where} \begin{bmatrix} w_{p1} \\ w_{M1} \\ w_{T1} \\ w_{p2} \\ w_{M2} \\ w_{T2} \\ w_{p3} \\ w_{M3} \\ w_{T3} \end{bmatrix}_t = \text{MVN}\left(0, \begin{bmatrix} q_p & 0 & 0 & 0 & 0 & 0 & 0 & 0 & 0 \\ 0 & q_M & 0 & 0 & 0 & 0 & 0 & 0 & 0 \\ 0 & 0 & q_T & 0 & 0 & 0 & 0 & 0 & 0 \\ 0 & 0 & 0 & q_p & 0 & 0 & 0 & 0 & 0 \\ 0 & 0 & 0 & 0 & q_M & 0 & 0 & 0 & 0 \\ 0 & 0 & 0 & 0 & 0 & q_T & 0 & 0 & 0 \\ 0 & 0 & 0 & 0 & 0 & 0 & q_p & 0 & 0 \\ 0 & 0 & 0 & 0 & 0 & 0 & 0 & q_M & 0 \\ 0 & 0 & 0 & 0 & 0 & 0 & 0 & 0 & q_T \end{bmatrix}\right) \quad \text{(A3a)}$$

for the state-process model and

$$\begin{bmatrix} y_{p1} \\ y_{M1} \\ y_{T1} \\ y_{p2} \\ y_{M2} \\ y_{T2} \\ y_{p3} \\ y_{M3} \\ y_{T3} \end{bmatrix}_t = \begin{bmatrix} x_{p1} \\ x_{M1} \\ x_{T1} \\ x_{p2} \\ x_{M2} \\ x_{T2} \\ x_{p3} \\ x_{M3} \\ x_{T3} \end{bmatrix}_t + \begin{bmatrix} v_{p1} \\ v_{M1} \\ v_{T1} \\ v_{p2} \\ v_{M2} \\ v_{T2} \\ v_{p3} \\ v_{M3} \\ v_{T3} \end{bmatrix}_t$$

$$\text{where} \begin{bmatrix} v_{p1} \\ v_{M1} \\ v_{T1} \\ v_{p2} \\ v_{M2} \\ v_{T2} \\ v_{p3} \\ v_{M3} \\ v_{T3} \end{bmatrix}_t = \text{MVN}\left(0, \begin{bmatrix} 0.007 & 0 & 0 & 0 & 0 & 0 & 0 & 0 & 0 \\ 0 & 0.10 & 0 & 0 & 0 & 0 & 0 & 0 & 0 \\ 0 & 0 & 0.30 & 0 & 0 & 0 & 0 & 0 & 0 \\ 0 & 0 & 0 & 0.007 & 0 & 0 & 0 & 0 & 0 \\ 0 & 0 & 0 & 0 & 0.10 & 0 & 0 & 0 & 0 \\ 0 & 0 & 0 & 0 & 0 & 0.30 & 0 & 0 & 0 \\ 0 & 0 & 0 & 0 & 0 & 0 & 0.007 & 0 & 0 \\ 0 & 0 & 0 & 0 & 0 & 0 & 0 & 0.10 & 0 \\ 0 & 0 & 0 & 0 & 0 & 0 & 0 & 0 & 0.30 \end{bmatrix}\right) \quad \text{(A3b)}$$

21508925, 2013, 5, Downloaded from https://esajournals.onlinelibrary.wiley.com/doi/10.1890/ES13-00019.1, Wiley Online Library on [22/01/2026]. See the Terms and Conditions (https://onlinelibrary.wiley.com/terms-and-conditions) on Wiley Online Library for rules of use; OA articles are governed by the applicable Creative Commons License

for the observation-process model, where the subscripted numerals denote the three pools (1, 2, and 3). Note that one set of parameters was used for all three pools to describe the between-species (and autoregressive) interactions and the effects of the covariates, hence why the terms in **B** and **C** do not include subscripted numerals. The final set of parameters, $\boldsymbol{\pi}$, were fixed but unknown and described the state variables at time $t = 0$, such that $\mathbf{x}_0 \equiv \boldsymbol{\pi}$:

$$\begin{bmatrix} x_{p1} \\ x_{M1} \\ x_{T1} \\ x_{p2} \\ x_{M2} \\ x_{T2} \\ x_{p3} \\ x_{M3} \\ x_{T3} \end{bmatrix}_{t=0} = \begin{bmatrix} \pi_{p1} \\ \pi_{M1} \\ \pi_{T1} \\ \pi_{p2} \\ \pi_{M2} \\ \pi_{T2} \\ \pi_{p3} \\ \pi_{M3} \\ \pi_{T3} \end{bmatrix}$$

Interpolation-extrapolation procedure used with the covariate data

As explained in the main text, modeling temperature and salinity as true covariates (rather than as additional state variables) requires having data on them for every date in the process model. To accomplish this, I simply linearly interpolated the data between observations. For example, if temperature on day t (the first sample date) was observed to be 20°C and on day $t + 3$ (the second sample date) was observed to be 24.5°C, then I assumed that temperatures on days $t + 1$ and $t + 2$ were 21.5°C and 23°C. The interpolated rate of change (in this example, 1.5°C/d) was calculated for each interval between sample dates.

Further, to relate populations at time $t + 1$ to covariate levels at time t (to match the time lag on which the populations affect each other), the covariate data must be shifted forward one day and the values at time $t = 0$ (the day before the first sample was taken) must be included to avoid dropping data. Here, I simply assumed that the rate of the first interpolation interval (between the first and second sample dates) applied to the window from $t = 0$ to $t = 1$, and used this rate to extrapolate the temperature at $t = 0$. Continuing with this example, I assumed that the temperature at time $t - 1$ (the day before the first observation, $t = 0$) was 18.5°C.

21508925, 2013, 5, Downloaded from https://esajournals.onlinelibrary.wiley.com/doi/10.1890/ES13-00019.1, Wiley Online Library on [22/01/2026]. See the Terms and Conditions (https://onlinelibrary.wiley.com/terms-and-conditions) on Wiley Online Library for rules of use; OA articles are governed by the applicable Creative Commons License

Appendix B

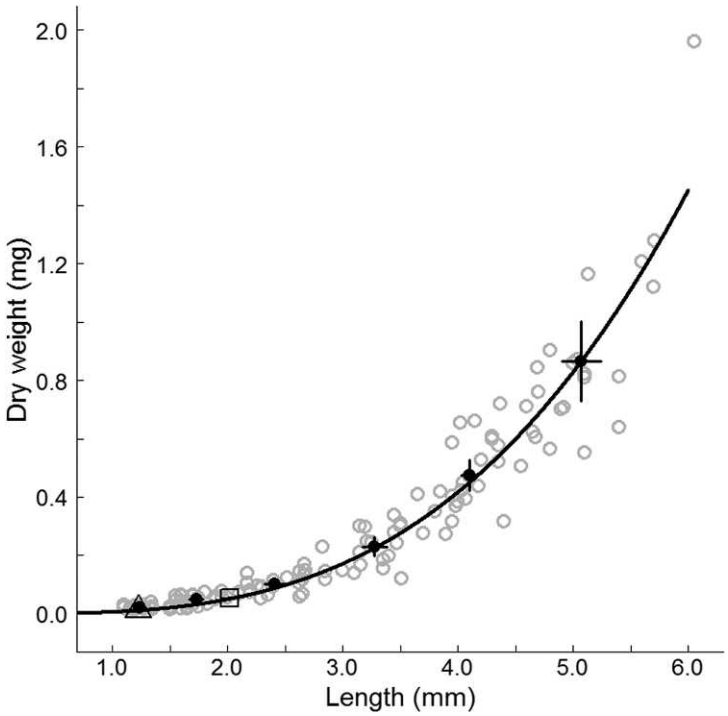

Fig. B1. Length-weight relationship for *Trichocorixa* (N = 132; 22 individuals from each of six instars). The grey open circles are individual data and the black filled circles are instar means with 95% CIs (the first-instar individuals are the smallest, and each subsequent instar is larger). The solid line is the length-weight regression fit to the individual data: dry weight = $0.0059 \times \text{length}^{3.078}$. The open triangle and square are the mean length-weight for *Moina* and *Daphnia* (respectively) used in the laboratory experiments.

21508925, 2013, 5, Downloaded from https://esajournals.onlinelibrary.wiley.com/doi/10.1890/ES13-00019.1, Wiley Online Library on [22/01/2026]. See the Terms and Conditions (https://onlinelibrary.wiley.com/terms-and-conditions) on Wiley Online Library for rules of use; OA articles are governed by the applicable Creative Commons License

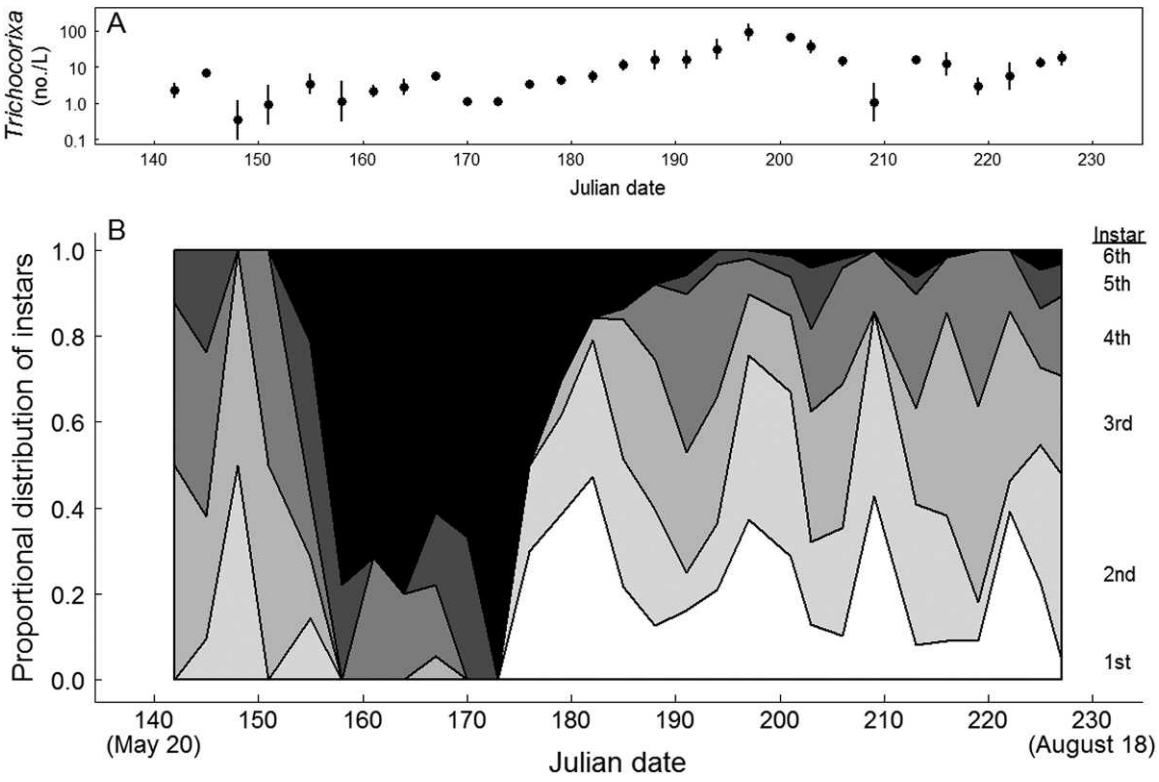

Fig. B2. Average numerical densities (A) and combined age distributions (B) of the three *Trichocorixa* field populations. Error bars in (A) are among-pool standard errors. In (B), successive instars are stacked on top of each other with darkness increasing with stage from white for first instar to black for adult.

21508925, 2013, 5, Downloaded from https://esajournals.onlinelibrary.wiley.com/doi/10.1890/ES13-00019.1, Wiley Online Library on [22/01/2026]. See the Terms and Conditions (https://onlinelibrary.wiley.com/terms-and-conditions) on Wiley Online Library for rules of use; OA articles are governed by the applicable Creative Commons License

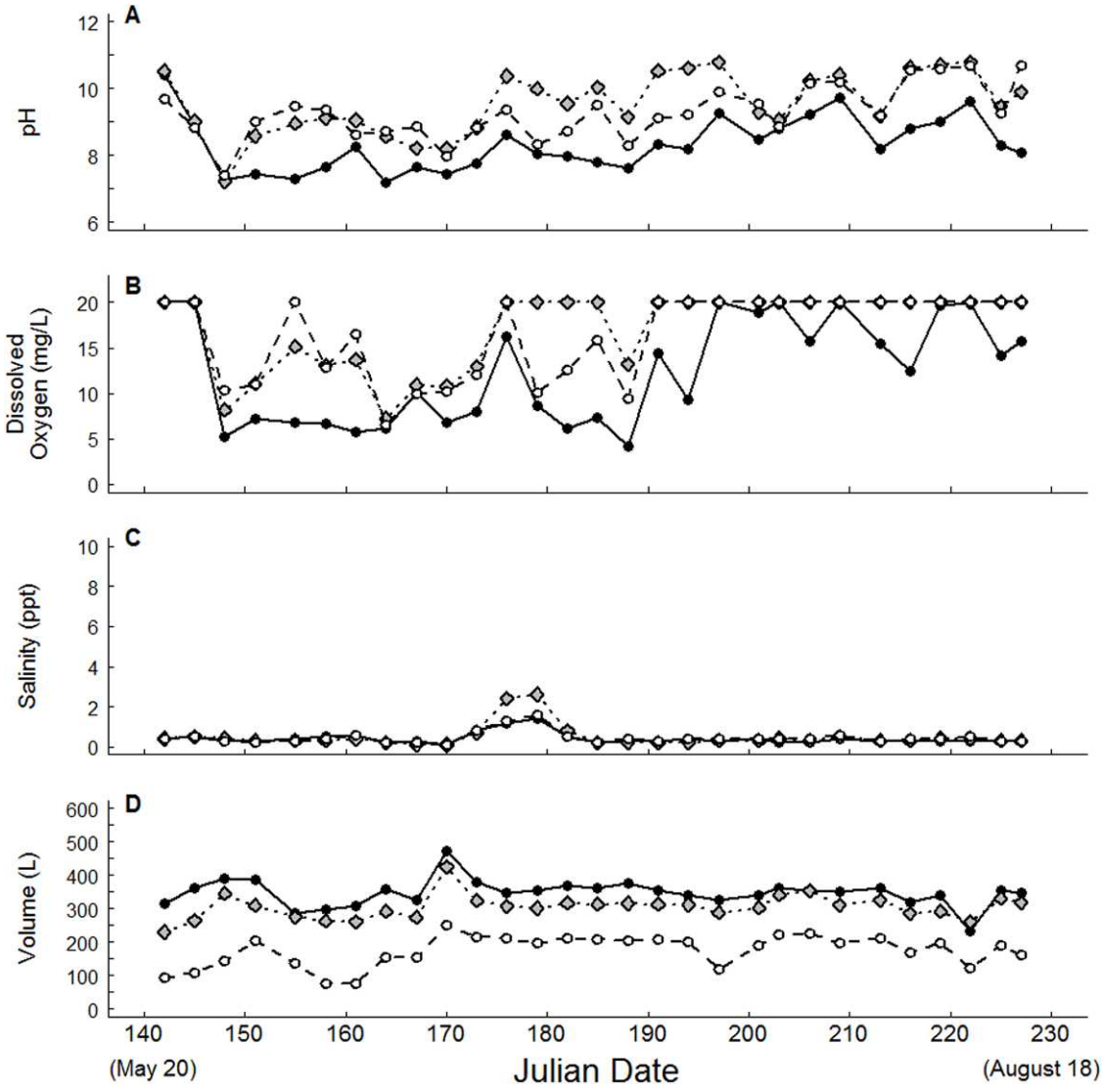

Fig. B3. Additional physicochemical data on the three pools shown in Fig. 4 in the main text (point and line types matching those in Fig. 4).

21508925, 2013, 5, Downloaded from https://esajournals.onlinelibrary.wiley.com/doi/10.1890/ES13-00019.1, Wiley Online Library on [22/01/2026]. See the Terms and Conditions (https://onlinelibrary.wiley.com/terms-and-conditions) on Wiley Online Library for rules of use; OA articles are governed by the applicable Creative Commons License